Second Response to the Comments of Reviewer 1

We are again grateful to reviewer 1 for his/her useful comments that helped us to improve our paper. In particular, an analysis following comment 34 provided a new insight into descent routes (see A34). Furthermore, the instructions for proper wording are very helpful for us, i.e., the non-native English speakers.

In this response, each comment is numbered like C1 etc. (Comment 1) and the corresponding answer is like A1 etc. (Answer 1). Pages and lines indicated are usually for those in the revised version. For convenience, the original comments from the reviewer are shown by blue color, responses by black color, and text in our revised paper by red color.

General Remarks

The paper has significantly improved. It is interesting and deserves publication. However, quite a few more amendments are necessary or should be considered:

Details

C1. Line 67: I suggest replacing "there" by "at high-lying sites" because work outside Tibet is cited.

A1. Our intention of "there" was not the Tibetan Plateau but mountainous areas. Anyway, corrected as suggested.

C2. Line 69: Better: "systematic deepest STT studies"

A2. Corrected as suggested.

C3. Line 70: Add "(e.g., Eisele et al., 1999)" as suggested before: here, some knowledge on the rare penetration into the PBL is summarized and a counter example is given.

A3. The observation site in Eisele et al., (1999) is the Zugspitze summit station. Therefore, its citation near l. 70 is not appropriate, because this paragraph generally describes the review of studies in non-mountainous areas. Since we think that "some knowledge", maybe, means what is written in Eisele et al., (1999), we did not mention that here. See also A34.

C4. Lines 74-75: "also investigated": I do not understand "also" since these references are not related to any work mentioned before in your text. This is a recent development in the U.S. related to air quality. I suggest removing "also".

A4. Before these papers are cited, a similar paper, Lin et al. (2012), is already cited.

Therefore, "also" is inserted here.

C5. Lines 76-78: Some statement like "Identifying the descent down to the surface is a challenge." is missing here. Then you can continue "Even in this study...".

A5. Based on the suggestion, corrected as "Identifying the descent down to the surface is a challenge. However, in these studies, the identification is insufficient, because air parcels originally in the stratosphere were not sequentially traced to the surface. Moreover, an indicator that directly demonstrated stratospheric intrusions to the surface was not used;" (ll. 78–81).

C6. Line 80: Add colon: "question: Can"

A6. Corrected as suggested.

C7. Line 83: Extend: "The problem is to find a way how "

A7. Corrected as suggested.

C8. Lines 83-89: This paragraph is not well written. It seems to suggest that trajectory calculations are the method of choice. Then this opinion is revoked. I suggest to jump directly into what has be done: "We decided to apply an approach based on both ....". H_2O would have been another good supporting tracer as one can see from the routine radiosonde measurements.

A8. We think this paragraph is important in the respect that the need of a different approach from the previous ones is written. Therefore, we rewrote this paragraph as follows: The problem here is how such a study can be conducted. It looks simple on the surface, because we can calculate forward trajectories of parcels originating in the stratosphere with the destination being Earth's surface, i.e., an extension of Wernli and Bourqui (2002), or backward trajectories in which the parcels originate at Earth's surface with the destination being the stratosphere. However, doing so is difficult: A trajectory between the stratosphere and surface has a longer completion time, as is clearly shown later. More importantly, most trajectories cannot reach the surface. In short, even if numerous trajectories are calculated, nearly all such calculations are of no use. (ll. 87–93)

In our preliminary inspection, H_2O was not a good supporting tracer in many cases, which is different from observations in the mountainous areas. Maybe, airmass from the stratosphere drifts for a few days near the surface where specific humidity is high. So we did not mention it.

C9. Line 97: "extended air travel durations"

A9. Corrected as suggested.

C10. Lines 98-99: "are not observed with": You certainly mean "are not provided by".

A10. Corrected as suggested.

C11. Line 102: "are put together".

A11. Corrected as suggested.

C12. Line 130: "is generally high" seems to be more an expectation than the result of that study as far as I remember. Please, have a look at that paper again.

A12. The abstract in Zanis et al. (2003) says "High ratio values are generally met under cyclonic or northerly advective conditions, which are the synoptic situations mostly related to stratosphere-to-troposphere transport (STT) events." Therefore, it was rewritten as "... is generally high under synoptic situations related to stratospheric intrusion episodes" (l. 136).

C13. Line 135: "By using ^{7}Be and H_2O thresholds ..."

A13. Corrected as suggested.

C14. Line 230: Move citation in the final sentence of this paragraph up to here and delete the final sentence.

A14. Corrected as suggested.

C15. Sec. 3.2 needs revision:

A15. By the changes from A16 to A20 and other corrections, subsection 3.2 was improved. Please check ll. 259–290 once more.

C16. Line 258: First of all the number of cases should be specified here, the total number of trajectories.

A16. Since we did not understand "the total number of trajectories" in this comment, this part was neglected. We understood "the number of cases" as the cases (times) in which backward trajectories were calculated. Then, the second sentence in this subsection was changed to "However, all of these times (267 times) were not objectives for analysis," (ll. 259–260).

C17. The role of $\hat{z}_1$ is unclear; where are the other $\hat{z}_i$ related to it?

A17. The role of $\hat{z}_1$ is to select the cases for analysis as one index, as well as $\hat{z}_a$. The other $\hat{z}_i$ ($i = 2, ...$), together with $\hat{z}_1$, are used to calculate $\hat{z}_a$ in (1) and to select trajectories to calculate the top-1% and top-25% averaged trajectoties in section 4.

In relation to the latter, we forgot to define $z_i(t)$ used in (2) in the previous versions. Then, we added the following sentence in section 4: Furthermore, $z_i(t)$ is defined as the trajectory with i-th highest altitude, which is a function of time, t. (ll. 294–295).

C18. Lines 261: "However, the ^{7}Be concentration does not necessarily correspond only to $\hat{z}_1$": why should it, why this sentence?

A18. We wrote the reason just after this sentence as "because even if $\hat{z}_1$ is high, the ^{7}Be concentration does not become high when, for example, the altitudes of all the other trajectories are low." (ll. 262–264 in the previous version). However, the part of "the ^{7}Be concentration does not become high" might give confusion: This "^{7}Be concentration" meant the obseved one at the surface, but it might be taken as the original concentration of the $\hat{z}_1$ route. Therefore, we rewrote it in the revised version as "However, the ^{7}Be concentration observed at the surface does not necessarily correspond only to $\hat{z}_1$, because even if $\hat{z}_1$ is high, the ^{7}Be concentration at the surface, which is observed as a somewhat mixture of air parcels originating from many trajectories, may not become high when all the other trajectories come from low altitudes." (ll. 267–271).

C19. Line 270: Why plural when there is just a single altitude, $\hat{z}_1$?

A19. One case has one $\hat{z}_1$, so the 47 cases mentioned above have 47 values of $\hat{z}_1$. Consequently, the plural is used here. We rewrote this sentence as "The maxima of the highest reached altitudes, $\hat{z}_1$, for these 47 cases are all more than 6000 m." (ll. 276–277).

C20. Line 277: "The case numbers... "

A20. Corrected as suggested.

C21. Line 303: "is the most important task"

A21. Corrected as suggested.

C22. Line 303: "... is investigated in Sec. 4.2.3."

A22. Maybe, Line 310. Corrected as suggested.

C23. Line 315: "maximum-descent"

A23. Corrected as suggested.

C24. Line 316: Do you mean "corresponds to"??? "Followed by" does not make sense.

A24. We are very sorry that "large descent" and "large latitudinal movement" should have been exchanged; that is, the right time sequence is "large latitudinal movement" $\rightarrow$ "large descent." This part was rewritten as "In Fig. 4, the maximum-descent paths (lines terminated by red symbols) are generally located at the low latitude side, compared with

the paths of the maximum latitudinal movement (black symbols), which indicate that the large latitudinal movement is followed by the large descent." (ll. 323–325).

C25. Line 317: "slow" seems to contradict the figures.

A25. "Slow" is compared with the large descent. To paraphrase, the latitudinal movement terminated by black symbols is accompanied by slow descent, compared with the large descent. This sentence was rewritten as "the latitudinal movement is accompanied by relatively slow descent." (ll. 325–326).

C26. Line 326: "the last two days of travel."

A26. Corrected as suggested.

C27. Line 343: "to reach finally" (no split infinitive, please)

A27. Corrected as suggested.

C28. Line 347: "Case studies"

A28. Corrected as suggested.

C29. Line 353: "Afterwards"

A29. Corrected as suggested.

C30. Line 356: "The features represented by this case are typical...."

A30. Corrected as suggested except "the" instead of "The".

C31. The paragraph starting at line 358 read much like there is a lot of mystery about the mechanism. Tropopause folding is quite normal. Please, rewrite in a more direct way.

A31. Even though tropopause folding is quite normal, it is necessary to explain in detail that tropopause folding is one mechanism of fast descent routes. Here, we must explain at least the following two points; the phenomenon is really tropopause folding and the air parcels along the trajectories ride on the downward motion associated with the tropopause folding. The former corresponds to "Near 65°N in Fig. 7b, the area with large PV hangs deeply into the troposphere. Because this feature is also seen in a longitude-vertical section (not shown), this phenomenon is considered a tropopause fold," and the latter corresponds to "Air parcels with large PV exist near this region, and weak subsidence is dominant at the northeast side of this disturbance. The parcels at high altitudes descend by this subsidence (Fig. 7b)." Thus, it seems to us that this paragraph is necessarily and sufficiently written.

In this sense, many analyses in previous studies, in particular, studies on surface ozone elevation, are insufficient, because they simply showed that a tropopause fold occurred before the surface ozone elevation, but did not show that the parcels associated with a tropopause fold are not traced to the surface.

C32. Line 399: "northerly air flow"?

A32. Since northerly wind is, maybe, more popular, "northerly" was replaced by "northerly wind" (l. 419).

C33. Line 403: Already written in line 356! I do not complain, but the authors should be aware. One could improve the sentence by starting "The similarity of the routed ....". Then it refers what was already said.

A33. We cannot understand that the sentences starting from line 403 are already written in the setence in lines 356–357 in the previous version: The latter is written for case 1, while the former is explained for the other cases.

We thank you for presenting how to improve this part. However, we do not know how to continue from "The similarity of the routed ....". Therefore, this sentence was rewritten as "The other cases attaining the highest altitude at high latitudes also show similar routes in the respect of the southward movement with slow descent along an isentropic surface followed by rapid descent at the southern edge of a developed trough (not shown)" (ll. 423–425), though almost the same.

C34. P. 14 or Sec. 5: As said before, I am missing a brief discussion on the penetration into the layer just above the ground (PBL during daytime). In a manuscript not yet published and in earlier work cited by Eisele et alc (1999) this is explicitly discussed. The results suggest that the penetration is almost impossible after the onset of convection. Even if a related study with your data would be beyond the scope of your paper a few words are mandatory.

A34. As mentioned in the previous reply, we still cannot identify where Eisele et al. (1999) discussed the mixing associated with the change of the PBL. Furthermore, it seems to us that this comment is inconsistent with the previous one that "a case of deep STT reaching low altitudes in the early morning followed by downward mixing in the developing PBL."

Anyway, we investigated the time (daytime and night-time) dependency of the behavior of air parcels in low altitude. The results are shown in Fig. 1 below. It is clear

from Fig.1a that parcels between about 500 and 1500 m descend fast at daytime, while they stay at relatively near-constant altitudes at night-time. We can also see from Fig. 1b that the fast descent is related to the almost constant potential temperature in the vertical direction at daytime, i.e., the daytime mixing. On the other hand, the potential temperature has a strong vertical contrast at night-time (not shown). The other cases also show similar features in general.

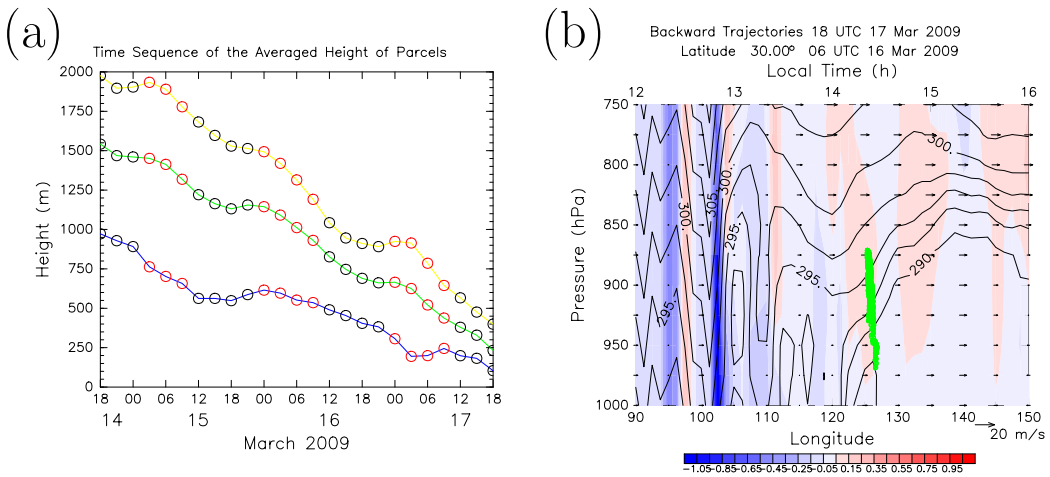

Figure 1: (a) Time change of the average heights of all the air parcels (green line), lowest-10% parcels (blue line) and highest-10% parcels (yellow line) on the trajectories for case 1. The ordinate is height, and the abscissa is time. The red and black circles indicate the average heights at daytime (8:00-20:00 Local Time) and night-time (20:00-8:00 Local Time), respectively. (b) Longitude-vertical section of the parcel positions (green circles), potential temperature (contour; unit: K) with a contour interval of 2.5 K, and vertical velocity (shading; unit: $\mathrm{Pa\,s^{-1}}$) along 30°N at 06:00 UTC 16 March 2009. The horizontal arrows show the zonal wind, and the local time (h) is indicated in the upper axis.

These results are worth presenting in the paper. Thus, we added this figure as Fig. 11 and one paragraph in pp. 12–13 (ll. 401–412): It is well known that the atmospheric boundary layer (ABL) shows a clear daily variation, in which the mixed layer develops during daytime, while the stable layer is formed during night-time. Therefore, the taking-in of air parcels above the ABL into the ABL must also show a daily variation.

Then, the time (daytime and night-time) dependency of the behavior of the air parcels on the trajectories entering the ABL is investigated. The results are shown in Fig. 11. Figure 11a illustrates that the parcels between about 500 and 1500 m rapidly descend at daytime, while they stay at relatively near-constant altitudes at night-time. Figure 11b indicates that the fast descent during daytime is closely related to the mixed layer (constant potential-temperature layer) extending to about 1500 m. On the other hand, the potential temperature has a strong vertical contrast at night-time (not shown). Thus, the air parcels above the ABL are easily taken into the ABL during daytime, while it is difficult for them to enter the ABL during night-time. However, the mixed layer has much smaller horizontal scales than the grid scale, a further analysis considering smaller scales is necessary.

We are very grateful to you for suggesting the difference in the role of the ABL between daytime and night-time. We expressed words of appreciation in the Acknowledgements.

C35. Lines 581-582: Fig. 22 does not give any idea of the mechanism that transports the air mass to the surface. Consider moving the introduction of the figure to the top of the paragraph. In general, as said, some of potential ideas about "These disturbances" are missing. How can trajectories work in the presence of daytime convection?

A35. The explanation of Fig. 22 was moved to the top of the paragraph, and the top of the paragraph was rewritten as "The majority of descent routes are from high latitudes and follow a particular sequence, as shown in Fig. 22: first, a descent..." (ll. 594–595).

"These disturbances" mean near-surface disturbances. As mentioned in ll. 343–345, near-surface disturbances have no specific form in the transport of air parcels to Fukuoka. This statement was reworded as "These disturbances occur in various forms" in the pevious version. "These disturbances have no specific form but various forms" is, maybe, clearer, and this expression was adopted in the revised version (ll. 603–604).

We cannot understand the last sentence, because nothing about "daytime convection" is mentioned in the results.

Figures:

Mark the position of Fukuoka (at least on busy figures where the geographical contour cannot be distinguished).

A. Black-filled circles were inserted at the position of Fukuoka in Figs. 7a, 8a, 8b, 9a,

9b, 15, 18a, and 18b. The figure numbers of 15 and 18 are those of 14 and 17 in the previous version.

Fig. 3, line 4: What "higher altitude"? Average of the upper percent? Highest in that ensemble.

5 A. We think that there is no "higher altitude" in the caption but, maybe, "highest altitude". More strictly, each symbol indicates the highest altitude of a top-1% averaged trajectory. We rewrote this sentence as "The symbol + shows the position of the highest altitude of each top-1% averaged trajectory" (ll. 3–4 in Fig. 3).

Second Response to the Comments of Reviewer 2

We are again grateful to reviewer 2 for his/her useful comments that helped us to improve our paper. In this response, each comment is numbered like C1 etc. (Comment 1) and the corresponding answer is like A1 etc. (Answer 1). Pages and lines indicated are usually for those in the revised version. For convenience, the previous responses are shown by magenta color, the original comments from the reviewer by blue color, responses by black color, and text in our revised paper by red color.

This is the review of a revised manuscript. The authors have addressed all the points that I raised in my previous review. Some of them have been adopted and others rejected. I do not know what other reviewers think about it, but the changes that authors have introduced in this new version are minor. They have got some improvements in the manuscript, but they seem unnecessarily combative with most of the ideas pointed out by the reviewers. Moreover they recognize lack of familiarity with the topic of STT exchange. Therefore I recommend taking more carefully the comments by the reviewers and accepting suggestions based on experience.

We are very sorry for your impression that we had a combative attitude to most of the ideas pointed out by the reviewers. Of course, we did not intend to do that, but intended to sincerely take all the comments into consideration. If you had such bad impression, it may be ascribed to our ability of English.

My recommendation is now 'Minor revision', but I suggest to the Editor that all my comments are taken into account before publication.

About your replies and other major comments:

==========

As to the evaluation of gnot too suprisingh, at least we were suprised at the following findings:

1. We discovered the mid-latutude route, which could not be expected. Also, the potential temperature sharply decreases along the trajectories of this route.

2. The high-latitude route is so systematic that the time sequence of descent by tropopause folding, southward transport by a strong trough, strong descent at the southern edge of the trough, and downward transport by appropriate near-surface disturbances is considerably regular for many cases.

3. There is a case (case 19) in which descent is as large as 6892m for two days, with

4659m recorded on the first day.

==>

C1. None of these is surprising to me. Maybe there are not too much existing literature on the topic, but being familiar with it includes a fair knowledge about what is obvious or at least a plausible and expected result.

A1. We cannot believe that the above items 1–3 are expected results. You may misunderstand the relationship between our results and the previous results mentioned below. (The possibility of the misunderstanding is stated below.)

C2. The latitude for FIHE and Boulder is similar. With your method you have found a far amount of trajectories with origin much poleward but you can not state that mechanisms are completely different in the studies of Wang and Polvani (2011) or Añel et al. (2012). Some differences are that Polvani et al. use a temporal domain of 17 days and Añel et al. (2012) use 10 days (as in your case). But different methods can provide slightly different results and this must be included for a balanced discussion of the topic.

A2. Although the latitude for FIHE and Boulder is similar, FIHE is a destination site at the surface of stratospheric air, while Boulder in Añel et al. (2012) is where the MT (multiple tropopause) or tropopause folding events occurs. That is, Boulder here is not a surface site. Therefore, it is useless to compare these two sites. Wang and Polvani (2011) also treated double tropopause events. Therefore, this paper also cannot be compared with our study. We are sorry that we cannot understand what you want to say here.

C3. In some way is striking to me the lack of conservation of PV and potential temperature. I think that it could be useful for readers if you include some extra discussion about this in the manuscript. That is, how the work with the data and computations drive to this result. In some way you have already highlighted it in the current version of your work, therefore probably your feeling is not too different of mine about this.

A3. We already explained in detail why the potential temperature is not conserved along the trajectories in subsection 4.2.2. We think no further explanation is necessary. We did not explain the non-conservation of PV, but it is easy to understand its reason, considering its small spatial scale.

==========

there is a striking systematic difference between MT events and the tropopause folds in

the present study, that is, occurrence frequencies show maxima in midltitude (i.e., zones of maximum cyclogenesis) in the former but in high latitudes in the latter. Pan et al. (2009) attribute MT events to latitudinal migration of the tropical tropopause over the extratropical one. Therefore, MT events may include not only tropopause folds but also other phenomena. In other words, MT events and tropopause folds do not correspond to one-to-one.

==>

C4. Fair enough. But then, are you considering foldings as the only way for STE?. Simply this is not true. Foldings are not the only way for stratospheric air reaching surface levels as I have already pointed out. Moreover, they should be really profound foldings and this is a low percentage of the total. Have you checked one-to-one that all your trajectories are related to synoptic-mesoescale systems of latitudinal and vertical dimensions letting such exchange? I do not recall seeing it in the manuscript, therefore if you make a generic statement about the potential causes, you must include a discussion broad enough to support the attribution of causes. Sure, tropical overlapping could disturb your results and drive to MTs in vertical soundings, but these cases are already removed with the analysis of trajectories. The point here is that a hot-spot for MT formation is probably related to a greater percentage of STE, lowering of the tropopause height and more effective mixing between layers. This facilitates STE (with independence of the tracer used) and it is what should be pointed out in the manuscript.

A4. Again, there seems some misundestanding. Although, of course, we do not think tropopause folding is the only way for STT, the point is what kind of STT participates in fast descent routes to the surface in Fukuoka. Our analysis indicates that the main participant is the tropopause folding in high latitudes. MT events presented in Añel et al. (2008) do not partipate in the present analysis in general, because MT events frequently occur in mid latitudes, while the high-latitude route is the majority in our analysis.

==========

The program that trajectories are pursued was made on our own, because the accuracy is very important in this study and free softwares are sometimes not fully accurate. However, similar trajectories could be traced by using any free softwares.

==>

C5. I guess that you have not clear the concept of 'free software'. Please, check

http://www.gnu.org/philosophy/free-sw.en.html
for a definition. 'Free software' has nothing to do with price and I think that you have not correctly understood it. If you have writen a piece of software (code) to perform the measurement work this is ideal. You should submit it as supplementary information, in this way everybody can check it and it can be included as part of the review process. The Creative Commons license used by ACP is compatible with software licenses and therefore of application.

A5. Certainly, we do not correctly understand the definition of free softwares.

We can submit our program written in FORTRAN. However, without a detailed explanation of how to use the program, general users cannot use it. Furthermore, the program is not general but specialized for the JRA-55 model grid data. The data are also special; they are not original GRIB data but sequential data for some special periods. Therefore, we think almost no one cannot use it, even if it is submitted.

C6. You also mention the use of the Dennou library. I have not been able of checking its license, but from the Ruby's version I guess that it could be a license from the BSD family. The Dennou library is included in the acknowledgements of other papers and you could do the same here, but I suggest passing it to the methods if you have a reference that you can use to cite and credit the developers.

A6. Thank you for your suggestion. However, we have never seen that the Dennou library is cited in References. So, this time, we want just to mention it in the acknowledgements.

Other minor points:

C7. I insist on my suggestion of including ^{7}Be in the title, I think that it is a strong point of the manuscript that will make it interesting for the scientific community and more read. As the authors are worried about the length of the title I suggest to remove 'fast descent routes' from the title. It is a concept hardly quantifiable from three words.

A7. "Fast descent routes" is a very important key word, because the elucidation of fast descent routes is the topic of the present study, and this word shortly represents its essence. Therefore, we cannot remove it. We agree with your opinion that the inclusion of ^{7}Be makes the title clearer. However, if including ^{7}Be, the title may be, for example, "Study on fast descent routes from within or near the stratosphere to Earth's surface in Fukuoka, Japan, with the use of high concentrations of ^{7}Be as an indicator." This title (28 words) seems too long. For comparison, the longest title among References is,

maybe, 20-word title. Then, we abandoned this title in the previous reply (Maybe, we should have presented this title explicitely in the previous reply). If you and the editor consider this length is acceptable, we are ready to change the title.

C8. lines 67-68: this is not true, Chen et al. 2013 study and shows with back trajectories and the synoptic-scale meteorological situation the mechanisms driving to this phenomenon. A more complete explanation of the feedbacks is provided in a paper recently accepted for publication in the Journal of Atmospheric Sciences (Chen et al. 2016, Reasons for the extremely high-ranging planetary boundary layer over the western Tibetan Plateau in winter, available in Early Online Releases). One of your replies to Reviewer 3 is about the work by Skerlak et al. (2014): you reasoning is that PBL is not equal to surface, but this depends a lot on orography. The works by Chen et al. (2011, 2013 and 2016) show clearly how STE to the PBL can be the almost the same than surface and in fact how the PBL can be considered to overshoot the tropopause. The problem right now in your manuscript is that you cite Chen et al. 2011 that is only a description. Maybe you could use the work of 2013 as I had recommended before. Probably what happened is that you mixed both studies after the study in 2011 was suggested by the Reviewer 1.

Please, have into account this full perspective when preparing a next version of the manuscript.

A8. We apologize that we did not cite Chen et al. (2013) in the previous version.

Features of STT, the atmospheric boundary layer, and therefore, descent routes from the stratosphere over the Tibetan Plateau are much different from those over non-mountainous areas, because the top of the mixed layer sometimes reaches more than 9000 m a.s.l.. Furthermore, since the object of this study is the clarification of descent routes to the surface in non-mountainous areas, a lengthy review about mountainous sites is unnecessary and rather undesirable. Therefore, we simply rewrote the last sentence of this paragraph as "However, since the top of the mixed layer sometimes reaches more than 9000 m a.s.l. over the Tibetan Plateau (Chen et al. 2013), features of STT and descent routes from the stratosphere are much different from those over non-mountainous areas." (ll. 68–70) as well as citing Chen et al. (2013, 2016)

C9. line 83: please, remove 'to have only'

A9. Removed.

C10. line 174: you state 'This period is sufficient for capturing the statistical character-

istics'. Being more correct probably what you mean is that a six years measurement period is a sample of the population enough to assume 'a priori' that the magnitude of the sampling error is acceptable. Therefore I suggest you to remove the sentence or rewrite it in a more accurate way.

A10. The sampling error is not serious because the error is only 5%. "Statistical characteristics" here have several meanings: Simple statistics include the average, variance, seasonal variation and so on of ^{7}Be. The most important is the statistics (for example, frequency and seasonal variation) of high concentration events of ^{7}Be. Because the six years are sufficiently long (the sample size is sufficiently large), these statistics can be obtained with a high degree of confidence. We simply rewrote this sentence as "This period is sufficiently long to capture statistical characteristics with a high degree of confidence." (ll. 180–181).

C11. line 274: the last word would be better 'could'

A11. Corrected as suggested.

C12. line 522: '6000 m'

A12. Corrected.

C13. line 707: the surname in the reference is 'Gimeno'

A13. Corrected.

Second Response to the Comments of Reviewer 3

We are again grateful to reviewer 3 for his/her useful comments that helped us to improve our paper. In this response, each comment is numbered like C1 etc. (Comment 1) and the corresponding answer is like A1 etc. (Answer 1). Pages and lines indicated are usually for those in the revised version. For convenience, the original comments from the reviewer are shown by blue color, responses by black color, and text in our revised paper by red color.

C1. I strongly suggest English revision by a professional translator or an English mother-tongue person.

A1. Before submitting the original manuscript, it was checked by a native English person, so the original parts may not be bad. Revised parts might be poor, but Reviewer 1 extensively corrected many bad expressions. Therefore, we think that this second revised version has a level of normal published papers.

If you or the editor think that the English level of this version is still low, we are ready to ask a native English speaker to make English revision.

C2. I'm still convinced that the tropopause folding selection methodology presented by Section 5.2 is rather rough compared with Sprenger et al. (2003). As stated by the authors, the reasons of the differences with Sprenger et al. (2003) are only speculative. This should be stressed in the paper.

A2. We are aware that the tropopause folding selection methodology presented in section 5.2 is rough. So we already wrote as "although this definition may be a bit exclusive, and it may apply to cases with no precise tropopause folding." (ll. 524–525 in the previous revised version). However, becuase our object is not to clarify tropopause folding itself, it is not unreasonable that the methodology is rough compared with methodologies in studies whose object is to clarify tropopause folding. We added the following sentence at the last in the paragraph in question: "Needless to say, a more detailed analysis of tropopause folding in high latitudes is necessary, because its definition adopted in this study is rough." (ll. 550–551).

C3. Finally, the investigation about the role of near surface distubances (Section 5.2) is rather weak in my opninion. Indeed, the authors considered just 1 year (2011) in comparing January and April back-trajectories. Since, I expect a kind of interannual variability in synoptic-scale transport, multi-year analysis is mandatory to support the

conclusions.

A3. Over Japan, the winter monsoon, in which the main wind direction is northwest, prevails in January, while extratropical cyclones and anticyclones are active in April. These features are consistent with what Figure 22 (21 in the previous version) shows. In other words, Figure 22 shows typical features in January and April. Therefore, it is not necessary to consider the interannual variability. Just to be certain, we performed similar numerical experiments for April in 2010 and 2013 and for January in 2010 and 2012 (because we already have data in these periods in hand without newly downloading from the JRA-55 site). The results are similar to Fig. 22, as expected. We added the following sentence: "These features in January and April are confirmed to be similar in other years. (l. 578).

Manuscript prepared for J. Name
with version 2015/09/17 7.94 Copernicus papers of the LaTeX class copernicus.cls.
Date: 19 April 2016

Fast descent routes from within or near the stratosphere to Earth's surface in Fukuoka, Japan

H. Itoh[1] and Y. Narazaki[2]

[1]Department of Earth and Planetary Sciences, Kyushu University, 744, Motooka, Nishi, Fukuoka, 819-0395, Japan
[2]Fukuoka Institute of Health and Environmental Sciences, 39, Mukai-Zano, Dazaifu, Fukuoka, 818-0315, Japan

Correspondence to: H. Itoh (itoh@weather.geo.kyushu-u.ac.jp)

Abstract. By using high concentrations of ^{7}Be as an indicator, we clarify fast descent routes from within or near the stratosphere to Earth's surface, with the study site being in Fukuoka, Japan. Most routes arise from high latitudes through the following processes. First, the descent associated with a tropopause fold occurs, followed by southward movement with slow descent at the rear side of a strong trough. Because this motion occurs along an isentropic surface, the descending air parcels nearly conserve the potential temperature. As an extension, a strong descent associated with a sharp drop in the isentropic-surface height occurs at the southern edge of the trough; this transports air parcels to low altitudes. This process involves irreversible phenomena such as filamentation and cutoff of potential vorticity. Finally, upon meeting appropriate near-surface disturbances, parcels at low altitudes are transported to Earth's surface.

In some cases, parcels descend within mid-latitudes. In such routes, because the potential temperature is much higher at high altitudes than at low altitudes, ~~strong~~ descent with conservation of the potential temperature is impossible, and the potential temperature decreases along the trajectories. In these cases, the entire flow does not move downward; instead, only part of the flow in a diffluent-wind field descends. ~~When~~ Because parcels descend, ~~they push~~ pushing low isentropic surfaces, ~~and~~ their potential temperature decreases upon mixing with parcels having low potential temperature in the lower layers.

The prevalence of the high-latitude route is explained as follows. In the mid-latitude route, because parcels at high and relatively low altitudes mix, the high concentrations of ^{7}Be included in high-altitude parcels are difficult to maintain. Therefore, for parcels to arrive at low altitudes in the mid-latitude while maintaining high concentrations of ^{7}Be, i.e., conserving the potential temperature, their area of origin should be high altitudes in high latitudes where the potential temperature is almost the same as that in the arrival area. Moreover, the initial descent must occur, because parcels cannot descend in the stratosphere when moving from high to mid-latitudes; parcels must already have descended from the stratosphere to the troposphere in high latitudes for effective descent with the movement to mid-latitudes.

In spring, tropopause folds are frequent in high latitudes, disturbances in the southward transport of parcels are strong, and disturbances occur by which parcels descend to the surface. Therefore, high concentrations of ^{7}Be occur most frequently in spring.

1 Introduction

Stratosphere-to-troposphere transport (STT) has attracted much research interest in the fields of atmospheric dynamics and chemistry and environmental science. Therefore, numerous studies have focused on STT since its investigations started in the 1950s (e.g., Reed and Sander, 1953; Machta, 1957). Thus far, the average features of the STT have been clarified considerably (Holton et al., 1995; Stohl et al., 2003; US Environmental Protection Agency, 2006, etc.). The intrusion of stratospheric air into the extratropical troposphere involves synoptic-scale and mesoscale processes among which tropopause folds and cutoff lows are the most important (Stohl et al., 2003; Sprenger et al., 2003, Nieto et al., 2008). However, many STT studies focused on stratospheric air infiltration to the troposphere, and, therefore, they only examined the transport process to the upper- and mid-troposphere.

Only recently, full-fledged studies on deep intrusions to the troposphere (deep STT) have been conducted, although, before the 2000s, there were several papers showing that stratospheric intrusions influence surface ozone (e.g., Oltmans and Levy, 1992). By using one-year reanalysis data from the European Centre for Medium-Range Weather Forecasts (ECMWF), Wernli and Bourqui (2002) obtained numerous forward trajectories to arrive below the 700 hPa level within a four-day period. As a result, it was confirmed that deep STT occurs frequently during winter and that its source regions are the storm tracks between 40 and 50° N. Furthermore, the geographical distribution of deep STT events was shown to be different from that of full sets of STT events. By extending the analysis period to 15 years, Sprenger and Wernli (2003) conducted similar analyses, the results of which nearly matched those of Wernli and Bourqui (2002). They further examined destinations, in which the maximum was shown to be along the west coast of North America. James et al. (2003a, b), by using a Lagrangian particle dispersion model, extended the considered time-scales and included transport processes such as convection and turbulence that were not included in the trajectory model. Škerlak et al. (2014) investigated deep STT by using 33 year ECMWF reanalysis data. According to their results, deep STT shows especially strong geographical and seasonal variations. The global hot spots for deep STT include the west coast of North America and the Tibetan Plateau, particularly in boreal winter and spring. However, in these studies, the descent mechanism was not examined.

Because the deepest area of the troposphere is above Earth's surface, a study of descending air from the stratosphere to the surface is very intriguing as "the deepest STT". Furthermore, if rapidly descending air from the stratosphere exists on the surface, it is interesting to note how this air is substantially and chemically different from general tropospheric air and what happens as a result from the perspective of atmospheric chemistry and environmental science. The surface in mountainous ar-

eas has similar height to 700 hPa or so. Therefore, there has been a growing number of publications in which destination sites are in mountainous areas, in particular, in the Tibetan Plateau or its vicinity (e.g., Cristofanelli et al., 2010; Chen et al. 2011; Bracci et al., 2012; ~~Ma et~~ Chen et al. 2013; Ma et al., 2014; Ohja et al., 2014; Chen et al. 2016). Backward trajectory analysis suggests that the position of the subtropical jet stream could play an important role in deep stratospheric intrusions (Cristofanelli et al., 2010). Impact of deep STT to atmospheric composition of not only ozone but also other atmospheric tracers has been investigated ~~there~~ at high-lying sites (Trickl et al., 2010; Bracci et al., 2012). However, ~~even in these studies, the descent mechanism was not fully examined~~since the top of the mixed layer sometimes reaches more than 9000 m a.s.l. over the Tibetan Plateau (Chen et al. 2013), features of STT and descent routes from the stratosphere are much different from those over non-mountainous areas.

In non-mountainous areas on the other hand, systematic deepest STT studies have not been conducted thus far. At most, studies have discussed whether surface ozone is influenced by stratospheric ozone. Lin et al. (2012) showed that a global high-resolution chemistry-climate model can capture the observed layered features and sharp ozone gradients of deep stratospheric intrusions. These stratospheric intrusions led to elevated background ozone concentrations. Ambrose et al. (2011), Lefohn et al. (2012), Langford et al. (2012), Yates et al. (2013), Langford et al. (2015), and Lin et al. (2015) also investigated influences of STT to elevated ozone concentrations at several stations in the USA, by using numerical models and aircraft and lidar observations. ~~However, even in this study,~~ Identifying the descent down to the surface is a challenge. However, in these studies, the identification is insufficient, because air parcels originally in the stratosphere were not sequentially traced to the surface. Moreover, an indicator that directly demonstrated stratospheric intrusions to the surface was not used; therefore, it is difficult to judge whether the result was actually influenced by stratospheric air.

In this context, the present study investigates the descending air from the stratosphere to Earth's surface in a non-mountainous area. This study aims at answering the following questions~~.~~: Can stratospheric air rapidly descend to the surface? If so, what route does it follow, and what mechanism is it based on?

The problem ~~here is~~ is to find a way how such a study can be conducted. It ~~only seems necessary to have only to obtain~~ looks simple on the surface, because we can calculate forward trajectories of parcels originating in the stratosphere with the destination being Earth's surface, i.e., an extension of Wernli and Bourqui (2002), or backward trajectories in which the parcels originate at Earth's surface with the destination being the stratosphere. However, doing so is difficult~~. As is clearly shown later, when the forward destination is the surface , the trajectory has a~~ : A trajectory between the stratosphere and surface has a longer completion time, as is clearly shown later. More importantly, most trajectories cannot reach the surface. In short, even if numerous trajectories are calculated, nearly all such calculations are of no use.

Thus, an appropriate indicator is required for effective trajectory calculations. In this study, we used the concentration of beryllium 7 (^{7}Be) as an indicator; ^{7}Be is a radioactive isotope, most of which (about 70%) is produced in the stratosphere (the remaining 30 % in the upper troposphere) by cosmic-ray spallation (Masarik and Beer, 1999; Nagai et al., 2000; Land and Feichter, 2003; Usoskin and Kovaltsov, 2008; Bezuglov et al., 2012), and it has a half-life as short as 53 days. Therefore, observations of high concentrations of ^{7}Be on the surface are direct indications of phenomena in which stratospheric air (or near-stratospheric air) promptly descends to the surface, because ^{7}Be decays during extended air travel durations in the troposphere, where high concentrations cannot be sustained. The two characteristics of stratospheric origin and short half-life time are unique to ^{7}Be and are not ~~observed with~~ provided by other substances. By setting the starting points and times of backward trajectories to the point at which high concentrations of ^{7}Be are observed, trajectory calculations can be conducted effectively. Note that, because high concentrations of ^{7}Be do not automatically guarantee stratospheric (or near-stratospheric) origins, other criteria are ~~set~~ put together, as described in ~~section~~ Sect. 3.

Numerous STT studies have employed ^{7}Be concentrations. However, when ^{7}Be is used alone, rapid descent might be missed because ^{7}Be concentrations become low when wet scavenging is performed on descending air (Gerasopoulos et al., 2001). Instead, the ratio of ^{10}Be to ^{7}Be is used (e.g., Raisbeck et al., 1981): ^{10}Be is also a radioactive isotope that is mainly produced in the stratosphere; however, its half-life time is 1.39×10^6 years, which is significantly longer. Thus, even when subjected to wet scavenging, the ratio is still small in rapid descent. However, for the purpose of this study, it is suffice to use ^{7}Be concentrations alone. This is because the objective is not to obtain all STT events and their statistical characteristics; instead, it suffices to consider a few tens of fast descent events. Missing some fast descents is not a weak point for the present purpose. In addition, as high concentrations of ^{7}Be are indicative of an absence of wet scavenging, it is simpler to trace backward trajectories in such cases, which is preferable for the present purpose.

In previous studies using ^{7}Be, its concentration was most often measured at mountain observatories in East Asia and Europe or through aircraft observations, and the STT was then studied using these data. In East Asia, Tsutsumi et al. (1998) measured the ozone and ^{7}Be concentrations at Mt. Fuji (3776 m a.s.l.) in Japan and found that both concentrations became large at some times. Backward trajectory analysis beginning at these times indicated the intrusion of a stratosphere-origin airmass into the troposphere. Zheng et al. (2011) observed ^{10}Be/^{7}Be on the Tibetan Plateau and found that it exhibited marked seasonal variations. By aircraft observations, Jordan et al. (2003) produced a large dataset of ^{7}Be concentrations. Upon analyzing this dataset, they inferred some STT mechanisms, including tropopause folds and mixing associated with subtropical jets. In Europe, Elbern et al. (1997) identified many stratospheric intrusion events at the two European summits, by using ^{7}Be and ozone concentrations. Stohl et al. (2000) combined ozone and ^{7}Be measurements on the Alps and northern Apennines and numerical-model calculations, investigating stratospheric

intrusions. In the project titled Influence of Stratosphere–Troposphere Exchange in a Changing Climate on Atmospheric Transport and Oxidation Capacity (STACCATO), combined measurements of ^{10}Be and ^{7}Be concentrations were carried out regularly during the course of a full year at two high-altitude stations (Stohl et al. 2003). In addition, the STT was studied on an integrated basis using several methods including numerical simulation. Zanis et al. (2003) showed that the $^{10}\mathrm{Be}/^{7}\mathrm{Be}$ ratio is generally high ~~during~~ under synoptic situations related to stratospheric intrusion episodes. Cristofanelli et al. (2003) and Usoskin et al. (2009) compared numerical model results with measured ^{7}Be concentrations at the surface, which revealed that all models captured the general behavior of the intrusion event. Cristofanelli et al. (2006) evaluated effects of stratospheric intrusions to surface ozone and ^{7}Be concentrations at the Mt. Cimone station (2165~~m a.s.l.~~ m a.s.l.) by calculating backward trajectories. By using a ^{7}Be ~~threshold~~and H_2O thresholds, Trickl et al. (2010) examined deep intrusions of stratospheric air reaching at the Zugspitze summit (2962~~m a.s.l.~~ m a.s.l.) in Germany. In summation, although the usefulness of ^{7}Be observations and numerical models for STT studies has been confirmed, no studies have focused on the access of stratospheric air to the surface other than that in mountainous areas, nor have its mechanisms been examined.

From the very start, it is impossible to present mechanisms from the aforementioned ^{7}Be observational data, except one data at the Mt. Cimone station (Cristofanelli et~~al.~~ al., 2006; Tositti et~~al~~ al., 2014). That is, in these data, sampling periods are long (one week or so) or observational periods are short (one year or less). Data from short sampling periods (one day or so) are required to narrow down the starting times of trajectory calculations, and extended consecutive observations are needed to provide generality to the proposed mechanisms. On the other hand, we have the necessary data in a non-mountainous area, which include short sampling periods and extended consecutive observations, as presented in Sect. 2. Thus, we can effectively perform numerous calculations of backward trajectories.

The remainder of this paper is organized as follows. In Sect. 2, the observational results of ^{7}Be concentrations are shown. In Sect. 3, high-concentration ^{7}Be events are extracted, and on the basis of this information, we propose a method for obtaining rapid descent routes using backward trajectories. In Sect. 4, we present the results and clarify the routes from the stratosphere to the surface. Moreover, the mechanism for fast routes is presented by specifying the phenomena associated with the routes. In Sect. 5, the discussions are presented. Finally, in Sect. 6, the conclusions are provided.

2 Observational results of ^{7}Be concentration

^{7}Be concentrations have been consecutively measured since 1998 (Narazaki and Fujitaka, 2009) at the Fukuoka Institute of Health and Environmental Sciences (FIHE) located in Dazaifu, Fukuoka Prefecture, Japan (33.5° N, 130.5° E, 30 m a.s.l.; Fig. 1). Sampling intervals are once every one to five days before March 2011 and nearly every day since then. However, measurements were not

available between 6 October and 19 November 2014, when the buildings were being retrofitted for earthquake resistance. The measurement times are around 00:00 UTC (09:00 Japan Standard Time). Among previous studies, only Kikuchi et al. (2009) examined the data of ^{7}Be concentration almost daily over several years at a non-mountainous site.

The ^{7}Be concentrations were measured as follows: aerosol samples were collected on quartz fiber paper (QR-100; 20.3 cm × 25.4 cm; ADVANTEC Co., Ltd.) using high-volume air samplers (HVC-1000N, HV-1000F, and HV-1000R; Shibata Science Co., Ltd.). The flow rate was 1000 L min^{-1}, and the integrated air volume was 1440–5500 m^3 per sample. The paper collecting the aerosol was folded with the sampling side inside to create 12 sheets that were then punched through by a punch with a diameter of 48 mm. To reduce their volume, the 12 sheets of paper were then pressurized with a force of about 10 t by a pressure machine to form a disk of 2 mm thickness. The ^{7}Be activity was measured using a high-purity germanium detector system (Canberra). The ^{7}Be concentrations were obtained after being adjusted to the sampling dates on which the radioactivity decayed with the half-life time of ^{7}Be. Error of ^{7}Be concentrations is typically 5%.

The analysis period is six years from 2009 to 2014. This period is ~~sufficient for capturing the statistical characteristics~~ sufficiently long to capture statistical characteristics with a high degree of confidence.

Figure 2 shows observational results of ^{7}Be concentrations. The measurement period is from April 2011, when the measurement was changed to once per day, to September 2014, prior to the earthquake-resistant retrofitting. The concentrations are quite low during summer, suggesting large seasonal variations. This result is the same as those reported by Megumi et al. (2000) and Kikuchi et al. (2009)[1] who presented observational results for other locations in Japan. However, Narazaki and Fujitaka (2009) also indicated several observational locations at which double peaks in spring and autumn are prominent.

Table 1 shows the seasonal averages and standard deviations (SDs) of ^{7}Be concentrations. Because the time resolution of the measurement is not constant, these values are calculated by considering the weight of time. DJF represents December, January, and February; MAM, March, April, and May; JJA, June, July, and August; and SON, September, October, and November. In the following, DJF, MAM, JJA, and SON are referred to as winter, spring, summer, and autumn, respectively, for simplicity. The averages are arranged by spring, winter, autumn, and summer in order of magnitude. However, because the differences are small except for summer, we consider the averages in spring, winter, and autumn to be nearly identical. The SDs are largest in spring, indicating a large time variation.

Peaks of ^{7}Be concentrations are observed in various seasons worldwide, and many studies have aimed at understanding how these peaks are determined (e.g., Feely et al., 1989; Buraeva et al.,

[1] Kikuchi et al. (2009) reported the existence of double peaks in spring and autumn. However, the concentrations in winter are nearly the same as those in spring and autumn, as far as we can see the figure.

2007). However, the focus of the present study does not require the identification of the factors determining seasonal variations.

3 Method for obtaining fast descent routes

3.1 Method and data

In this study, ^{7}Be concentrations of more than $10\,\mathrm{mBq\,m^{-3}}$ are defined as high-concentration events. $10\,\mathrm{mBq\,m^{-3}}$ is more than the average $+2$ SDs ($9.58\,\mathrm{mBq\,m^{-3}}$) from Table 1; therefore, this value is statistically significant (see also Fig. 2). Because the measurement time (starting and closing times of measurement) is around 00:00 UTC, high-concentration days are used almost interchangeably with high-concentration events.

At certain times on these days, it is highly possible that parcels originating from within or near the stratosphere arrive in Fukuoka, where Fukuoka refers to the area around FIHE in this study. We then calculated the backward trajectories from the five time points of 00:00, 06:00, 12:00, 18:00, and 24:00 (i.e., 00:00 on the following day) UTC on these days. These times are the output times for the Japanese 55 year Reanalysis (JRA-55) data. More specifically, the trajectories were traced from 1734 starting points near FIHE, which are on six levels (in intervals of 25 m from 25 to 150 m altitude above the surface), and 17×17 grid points with a grid interval of 5 km centered at FIHE on one altitude surface. Numerous starting points are used for three reasons. First, the ^{7}Be concentration at FIHE is not necessarily determined by one trajectory over FIHE but by many trajectories near FIHE, because diffusion is strong in the boundary layer. Second, the amount of air descending from the stratosphere can be evaluated from numerous trajectories. Third, to form clear statistical characteristics, numerous trajectories are needed. If the trajectories reach the stratosphere or its vicinity within 10 days, they are considered to exhibit fast descent routes from the stratosphere to Fukuoka. Moreover, we can present the mechanism of fast descent routes by specifying the meteorological phenomena occurring at these times.

The parcel positions were calculated by using the fourth-order Runge–Kutta scheme; the integration time step and period were 10 min and 10 days, respectively, and the wind, which advects the parcels, was interpolated linearly in time and in the vertical direction and by cubic splines in the horizontal plane. We assume that parcels were transported latitudinally and longitudinally by the meridional and zonal wind components, respectively. However, because such calculations cannot be conducted near the pole, they were performed in the following manner: first, the near-pole area was defined as the area north of 89.57° N, which is the northernmost Gaussian latitude. This spherical area was approximated as a plane, and the zonal and meridional winds were converted to the two components perpendicular to each other within this plane. The parcels were assumed to be advected by these wind components. The vertical motion is expressed by the vertical p velocity. Therefore,

parcel positions were first calculated in the pressure value, and then, by using the pressure and height data, the height value was obtained.

The model-grid data for the JRA-55 served as the meteorological data to trace the backward trajectories ~~.~~ (Kobayashi et al. 2015). Moreover, we used the isentropic and pressure-level data to specify the phenomena associated with the descent routes. In the model-grid data, the horizontal resolution is about 0.5625° (640×320 Gaussian grids) except near the poles, where the data grids are reduced. The number of vertical levels is 60 with a top level of about 10 Pa. The pressure-level data have a resolution of 1.25° in the longitudinal and latitudinal directions and 37 vertical levels, of which 23 levels below 200 hPa were used for the analysis. In the isentropic data, the two datasets in which the resolutions are the same as the model-grid data and 1.25° were used. The number of vertical levels is 21, of which only eight levels below the 340 K surface were used (the lowest level is the 270 K surface). ~~Details of the JRA-55 data are explained in Kobayashi et al. (2015).~~

High-concentration events of ^{7}Be are shown in the second row in Table 2. The total number of events was 43, covering 56 days. However, we should be cautious that the sampling intervals, i.e., averaging periods are not constant, because a longer averaging period relates to statistically fewer high-concentration days. Therefore, prior to March 2011, the high-concentration days may be underestimated. However, this difference is not considered in the present study.

Seasonal variations show that high-concentration days are predominant in spring (March, April and May), totaling 41 days (73 %). Two events in summer, on 1 and 2 June, should essentially be regarded as May events. If these are added to spring events, the appearance ratio in spring becomes 77 %. Following spring, seven winter events (nine days) are found. As the averaged concentrations are nearly the same among winter, spring and autumn, as observed previously, this means that the rapid descent routes from the stratosphere to Fukuoka occur frequently only in spring. The reason for such a large number of high-concentration days in spring is discussed in Sect. 5.

3.2 Case selection for analysis

As stated above, backward trajectories were traced from the five times over one day. However, all of these times (267 times) were not objectives for analysis, because among the five times, all trajectories could originate in altitude ranges other than the stratosphere and its adjacent region. Therefore, in this subsection, we simply explain how to select cases for analysis. The detail is described in the supplementary material.

First, two indices are defined. The first is $\hat{z}_1$ defined as follows. Let $\hat{z}_i$ $(i = 1, \ldots, 1734)$ be the highest altitude reached in each trajectory, where i is a suffix in order of the altitude. Therefore, $\hat{z}_1$ is the highest altitude among all 1734 trajectories. Because this value is, of course, one index to determine the parcel origin, $\hat{z}_1$ is the first index used to select object times for analysis. However, the ^{7}Be concentration observed at the surface does not necessarily correspond only to $\hat{z}_1$, because even if $\hat{z}_1$ is high, the ^{7}Be concentration ~~does~~ at the surface, which is observed as a somewhat mixture of air

parcels originating from many trajectories, may not become high when ~~, for example, the altitudes of~~ all the other trajectories ~~are low~~ come from low altitudes. Then, as the second index, we use the top-1 %, i.e., top-18 average of $\hat{z}_i$. This value is represented as $\hat{z}_\mathrm{a}$. That is,

$$\hat{z}_\mathrm{a} = \frac{1}{N_\mathrm{a}} \sum_{i=1}^{N_\mathrm{a}} \hat{z}_i, \tag{1}$$

where $N_\mathrm{a} = 18$. Objects for analysis are basically selected as the time when $\hat{z}_\mathrm{a}$ is the maximum and $\hat{z}_1 \geq 8000\,\mathrm{m}$.

Based on the maximum of $\hat{z}_\mathrm{a}$ only, 47 cases are selected, as shown in the third row of Table 2. The maxima of the highest reached altitude, $\hat{z}_1$, for these 47 cases are all more than 6000 m. However, in 14 cases among them, $\hat{z}_1$ is less than 8000 m; the remaining 33 cases, which are considered as reaching the stratosphere or adjacent regions, are chosen as objects for analysis. Among the objects for analysis, $\hat{z}_1$ of more than 10 000 and 9000 m is attained in 5 and 14 cases, respectively. Even in the 14 cases ~~less than~~ of $\hat{z}_1 <$ 8000 m, if the tracing times of backward trajectories were extended, the trajectories ~~would~~ could reach altitudes higher than 8000 m. However, this type of research is beyond the scope of the present study.

The details of the 33 cases are shown in the supplementary material. ~~Case~~ The case numbers are assigned in chronological order. The maxima of the potential vorticity (PV) of parcels on trajectories have all more than 2 PVU ($10^{-6}\,\mathrm{m^2\,s^{-1}\,K\,kg^{-1}}$); the minimum is 2.35 PVU and 30 cases exceed 3 PVU. Because 2 PVU is said to be an index of stratospheric air (e.g., Hoskins et al., 1985; Wernli and Bourqui, 2002; Sprenger and Wernli, 2003), all cases have the characteristic of stratospheric air in terms of PV. As PV is not well conserved (not shown), the Lagrangian time changes of PV are not mentioned in the following analyses.

4 Results

In this section, the terms "top 1 %" and "top 25 %" are frequently used. Their meanings are the same as those in the previous section, i.e., top 1 and 25 % of $\hat{z}_i$, the highest reached altitude, of each trajectory. Furthermore, $z_i(t)$ is defined as the trajectory with i-th highest altitude, which is a function of time, t. For simplicity, $\hat{z}_i$ or the highest reached altitude is omitted hereafter.

4.1 Overall characteristics

Figure 3 shows top-1 % averaged trajectories for two days from their highest altitudes for all the 33 cases. The averages of latitude and longitude were not obtained as the simple arithmetic averages of latitude and longitude but as averages of points on a sphere. The average in altitude was

$$\overline{z}(t) = \frac{1}{N_\mathrm{a}} \sum_{i=1}^{N_\mathrm{a}} z_i(t). \tag{2}$$

The highest altitude in the average trajectory is the maximum of $\overline{z}(t)$. This value is generally smaller than $\hat{z}_{\mathrm{a}}$. If the top-1 % trajectories vary widely among each other, the average trajectory is meaningless. However, because such cases are few, we consider that the overall features of descent routes can be captured.

Figure 3a shows that the longitudes of the trajectories vary among cases and do not have a strong tendency, although most trajectories attain the highest altitude in the eastern hemisphere. Conversely, trajectories in Fig. 3b show systematic motion in latitude and altitude. That is, the highest altitudes are located at high latitudes for many trajectories, and the altitudes lower as one moves to mid-latitudes. More specifically, with the exception of case 7, all cases attain their highest altitudes north of 45° N, and 25 cases attain them north of 60° N, i.e., in high latitudes. Thus, the routes from high latitudes are the main descent routes. The clarification of this mechanism is the ~~major problem~~ most important task in this study. Figure 3b shows that parcels lower the altitude while conserving their potential temperature in many cases. However, in case 7 and in a few other cases, the potential temperature is changed. Also in this respect, the characteristics of case 7 differ from those of many other cases. Case 19 shows a large descent of 6892 m for two days, with 4659 m recorded on the first day. The cause of this rapid descent is investigated in ~~the next subsection.~~ Sect. 4.2.3.

To pursue the route from high latitudes, we further examine the 25 cases in which the highest altitude is attained north of 60° N. Figure 4 shows the paths of the maximum latitudinal movement and maximum descent per day for these 25 cases. The maximum latitudinal movement per day means that moving distance per day in the southward direction is the maximum along a trajectory. The maximum descent per day has a similar meaning. Table 3 presents the times when these values are reached, along with the highest altitude, as the time from the starting time of backward trajectories. In Fig. 4, the ~~maximum descent~~ maximum-descent paths (lines terminated by red symbols) are generally located at the ~~lower~~ low latitude side, compared with the paths of the maximum latitudinal movement (black symbols), which indicate that the large ~~descent~~ latitudinal movement is followed by ~~large latitudinal movement~~the large descent. Furthermore, the ~~movement to the lower latitude~~ latitudinal movement is accompanied by relatively slow descent. According to Fig. 4 and Table 3, the following processes occur in the usual time sequence (forward trajectory): first, the highest altitude is achieved (its time is denoted as t_{a}). Slightly more than two days later, a large movement in the latitudinal direction begins with slow descent (start time: t_{m}), and slightly little less than two days after that, the largest descent occurs (start time: t_{d}). Because $t_{\mathrm{a}} - t_{\mathrm{m}}$ and $t_{\mathrm{m}} - t_{\mathrm{d}}$ are positive even at the edges of the confidence intervals of 99 % (26.7 and 17.7 h), the reversal of these times does not occur statistically. In fact, the reversal occurs only in a few cases, i.e., in three cases for $t_{\mathrm{a}} - t_{\mathrm{m}}$ (within three hours for all three cases), and only in one case (case 24) for $t_{\mathrm{m}} - t_{\mathrm{d}}$ among all ~~24~~25 cases.

Figure 5 shows the top-1 % averaged trajectories for the last two days of travel. At a glance, these trajectories are not systematic and approach Fukuoka from all directions. The variations in height

and latitude are small for two days, and a relatively long time is needed to finally arrive at Fukuoka at low altitudes, with the exception of three cases (cases 9, 23, and 31). These results are consistent with those in Table 3 in that it takes an average of 91 h (115.0 − 24.0) to reach the surface after the largest descent. Therefore, a long time is generally required to reach the surface from low altitudes such as 700 hPa, which is the destination given by Wernli and Bourqui (2002) and others. Thus, almost all calculations of backward and forward trajectories without an indicator would be of no use, as stated in the Introduction.

Disturbances affecting the arrival to the surface vary among cases, e.g., descending current associated with anticyclones and downward flow at the southwest side of extratropical cyclones. That is, no specific disturbance is involved in the transport of air parcels to Fukuoka; however, good matching between the parcel positions a few days prior to their arrival at Fukuoka and the disturbances is necessary.

In summary, the majority of the high-latitude routes take the following paths with a few exceptions. First, after attaining the highest altitude, air parcels descend slightly at high latitudes, followed by large movement toward low latitudes with slow descent. Then, a large descent occurs. From low altitudes, various disturbances are attributed to the long time required for the parcels to ~~finally reach~~ reach finally the surface.

In the following subsection, we examine in detail the mechanism for the high-latitude route, and we analyze a few characteristic cases other than this route.

4.2 Case ~~study~~studies

4.2.1 Descent routes from high latitudes

As stated in the previous subsection, the main route is the descent from the high latitudes north of 60° N. The mechanism of this route is clarified first.

Case 1 (starting time of 18:00 UTC 17 March 2009) is considered typical. Figure 6 shows the top-1% trajectories. With a few exceptions, the trajectories attain their highest altitudes about 10 days before the starting time of the backward trajectories (18:00 UTC 7 March). ~~Afterward~~Afterwards, air parcels descend to about 7000 m at 65–75° N, then moving to mid-latitudes with slow descent from about 18:00 UTC 10 March. Subsequently, they descend rapidly, and a long time is required to reach the surface from about 2500 m. In short, ~~this case shows features~~ the features represented by this case are typical of the descent route from high latitudes.

The first inspection is devoted to the mechanism of the descent from the highest altitude. Figure 7 shows the 300 hPa surface at 18:00 UTC 7 March (the last time of backward trajectories), and the vertical section of PV along 45° E 6 h later. The air parcels on the trajectories are also plotted to reveal their relationship with the trajectory. This time is chosen to represent the point at which the parcels on the trajectories record the highest altitude. Near 65° N in Fig. 7b, the area with large PV

hangs deeply into the troposphere. Because this feature is also seen in a longitude-vertical section (not shown), this phenomenon is considered a tropopause fold. Air parcels with large PV exist near this region, and weak subsidence is dominant at the northeast side of this disturbance. The parcels at high altitudes descend by this subsidence (Fig. 7b)[2]. This is the mechanism of the initial descent from the stratosphere.

Next, the mechanism of the southward movement with slow descent is revealed. Figure 8 shows the disturbance involved in the movement of parcels at 18:00 UTC 10 March ~~,~~ when the southward movement begins, and at 18:00 UTC 11 March, one day afterwards. It is clear that parcels are located on the rear side of a developed trough accompanied by strong southward wind. At 18:00 UTC 11 March, the trough develops further, as indicated by the change in the tilt of the trough axis from N–NE to S–SW. The slow descent is closely related to the downward inclination to the south of the isentropic surface: Fig. 9a shows the height and wind at the 300 K isentropic surface at the same time as that in Fig. 8b. The height decreases toward the south so that parcels necessarily descend with the southward movement, if the potential temperature is conserved. In fact, Fig. 6b reveals that conservation is achieved.

The rapid descent can be attributed to extension of the southward movement. At the southern edge of the trough, the height on the isentropic surface decreases dramatically (Fig. 9). In the case of weak troughs, streamlines could head north and upward after turning near the southern edge. In fact, we calculated forward trajectories in the case of weak troughs, confirming such movement (not shown). However, in this case, the trough axis indicates the tilt from N–NE to S–SW (Fig. 8b); therefore, the parcels are transported in a different direction from the moving direction of the system. ~~Therefore~~Thus, the parcels cannot move along with the system; that is, they cannot turn around the southern edge of the trough, and the altitudes of the parcels decrease dramatically (Figs. 9b and 6b). This irreversible process is closely related to the filamentation of the PV, as shown in Fig. 9b (Hoskins et al., 1985). When considering this event at a constant pressure level, we see that strong downward flow is dominant, and parcels descend under this flow, as shown near 120° E in Fig. 10. Subsequently, the parcels lag far behind the trough system and drift at low altitudes (not shown).

Finally, a near-surface disturbance is necessary for air parcels to reach the surface. In this case, it is a trough over the Sea of Okhotsk. Air parcels located around the subsidence region in the southern edge of the trough descend with eastward movement, arriving at Fukuoka (not shown).

It is well known that the atmospheric boundary layer (ABL) shows a clear daily variation, in which the mixed layer develops during daytime, while the stable layer is formed during nighttime. Therefore, the taking-in of air parcels above the ABL into the ABL must also show a daily variation. Then, the time (daytime and nighttime) dependency of the behavior of the air parcels on the trajectories entering the ABL is investigated. The results are shown in Fig. 11. Figure 11a illustrates that the parcels between about 500 and 1500 m rapidly descend at daytime, while they stay at

[2]Ascending parcels are those entering near 45° E from the west, as seen in Fig. 6a.

relatively near-constant altitudes at nighttime. Figure 11b indicates that the fast descent during daytime is closely related to the mixed layer (constant potential-temperature layer) extending to about 1500 m. On the other hand, the potential temperature has a strong vertical contrast at nighttime (not shown). Thus, the air parcels above the ABL are easily taken into the ABL during daytime, while it is difficult for them to enter the ABL during nighttime. However, the mixed layer has much smaller horizontal scales than the grid scale, a further analysis considering smaller scales is necessary.

Case 3 is presented as another case of the high-latitude route with a starting time of 06:00 UTC 3 May 2009 (Fig. 12). Although the positions of air parcels 10 days before the starting time and behaviors at low altitudes are different from those in Fig. 6, Fig. 12b is similar to Fig. 6b. That is, it shows the sequence of the descent at the initial time, southward movement with slow descent, and rapid descent, and the potential temperature is conserved in this sequence. Although figures are not shown, closer inspection shows that the same processes as in case 1 are involved: the initial descent is associated with a tropopause fold, the southward movement is accompanied by the northerly wind at the rear side of a developed trough, and the rapid descent is associated with the large drop in height at the southern edge of the trough. The only difference is that a cutoff low is included as an irreversible process in the last process.

~~Other~~ The other cases attaining the highest altitude at high latitudes also show similar routes ~~such as the~~ in the respect of the southward movement with slow descent along an isentropic surface followed by rapid descent at the southern edge of a developed trough (not shown). The behaviors of the air parcels near the ABL top during daytime and nighttime are also similar in general. Although a tropopause fold is also seen in many cases, it is not always included. In particular, in the case of $\hat{z}_1$ of about 8000 m at the initial, the parcels seem to be directly transported southward with no initial descent. Even in these cases, tropopause folds may occur before the last time of backward trajectories, but this is left as future work.

4.2.2 Descent routes within mid-latitudes

Figure 13 shows backward trajectories starting at 18:00 UTC 25 December 2009 (case 7), which is an example of the descent from high altitudes at mid-latitudes. We can clearly see that the potential temperature is not conserved; instead, it decreases. This decrease is expected: because the potential temperature at high altitudes is high, air parcels conserving potential temperature cannot fall from those positions to the surface where the potential temperature is low. Moreover, the top-1 % averaged route is largely different from the top-25 % averaged route. That is, the top-1 % trajectories are unique among the top-25 % trajectories; they are not representative of trajectories reaching relatively high altitudes. In these respects, the mid-latitude route differs from the high-latitude route.

We first explain why the potential temperature decreases with descent. Figure 14 shows the potential temperature and parcel positions on backward trajectories at 18:00 UTC 16 December. The time is just before the marked descent. The potential temperatures of air parcels have various values,

which ultimately mix[3]. Because the number of parcels with high potential temperature at high altitudes is relatively small, the potential temperature is not conserved and decreases. The fact that the top-1 % averaged route differs from the top-25 % is a manifestation of this mixing.

However, the reason for such mixing is still poorly understood. Then, the relationship between the parcel positions on trajectories and the horizontal pattern on an isentropic surface is shown in Fig. 15. The area near air parcels at high altitudes (the area near 40–45° N and 60–75° E) corresponds to a diffluent-wind area associated with a blocking high (area of low height nearly coincides with the blocking high; not shown), and the northward and southward flows with descent are split. The parcels on the trajectories ride on the southward flow of these two flows. That is, descending parcels are not most of the parcels coming from the west but parts of them, because the other parts ride on the northward flow. Moreover, Fig. 16 shows that descending parcels push isentropic surfaces (moving direction of air parcels and isentropic surfaces are not parallel). Therefore, many parcels do not descend as a whole; rather, only parts of them descend as the isentropic surfaces are pushed. For such descent, descending parcels are easily mixed with parcels having low potential temperature, which originally exist in lower layers in which descending parcels arrive.

Compared with these characteristics, we reconsider the reason for the conservation of the potential temperature in the high-latitude route. The flow in the high-latitude route is along an isentropic surface. Therefore, all parcels head southward; that is, they face the same direction. This characteristic allows the potential temperature to be conserved in the high-latitude route.

Other than case 7, all top-1 % trajectories of cases 5 and 26 show the mid-latitude route. In these parcels on the trajectories as well, only a part of the flows descend from a diffluent-wind field, pushing isentropic surfaces, although the characteristic of a ~~blocking high~~ blocking-high accompaniment is not seen.

4.2.3 Other characteristic routes

Figure 17 shows the top-1 % backward trajectories of case 19 (starting time of 12:00 UTC 16 May 2011), which is an example showing the rapid descent illustrated in Fig. 3. As the highest altitude reached in the average route is attained near 50° N (Fig. 17b), this case is not classified as a high-latitude route even though the parcels actually originate from high latitudes. However, unlike general cases of the high-latitude route, the trajectories do not show slow descent with southward movement; instead, they move to about 50° N while maintaining almost constant altitude. This occurs because this movement is associated with the extension of the polar vortex southward to the Altai-Sayan region (around 90°E and 50°N) rather than with the flow at the rear side of a trough (not shown). ~~Since~~ Because this process is also the cut-off of strong PV near the polar region, it can be grasped as the southward movement of tropopause folding (not shown. see also Fig. 18b). After that, the

[3]Strictly speaking, parcels themselves do not mix; instead, they approach each other. However, the distances among them are less than the grid length; thus, we express this state as “mixed”. Similar expressions are used below.

parcels descend rapidly. Because this descent from high altitudes to low altitudes occurs within the mid-latitudes, the potential temperature is not conserved along the trajectories (Fig. 17b), as in case 7.

The most interesting point in this case is its fast speed of descent of 4659 m per one day and 6892 m per two days. Figure 18 shows the horizontal pattern and parcel positions of the trajectories just prior to the large descent. The parcels showing large descent are located near 50° N and 105° E. Figure 18a shows that the parcels are located south of a diffluent-wind field. Furthermore, the potential temperature is high at both its south and east sides; thus, the gradient of the potential temperature is large in both directions. Considering this situation in terms of the isentropic surface, the height decreases dramatically in the direction of parcel movement. In fact, as confirmed by Fig. 18b, the height decreases by more than 4000 m at the southeast side where the parcels actually move. Moreover, the parcels exist in a diffluent-wind field, and their downward motion pushes isentropic surfaces. Consequently, parcels with high potential temperature at high altitudes mix with parcels having low potential temperature at lower altitudes, leading to a decrease in the high potential temperature. By repeating this process, parcels that are originally at high altitudes descend to low altitudes. These facts and considerations indicate that parcels exist in the strong-subsidence region on an isobaric surface (Fig. 18a) and experience rapid descent.

5 Discussion

5.1 Reason that the high-latitude route is the majority

In the previous section, it is shown that the descent route from high latitudes is dominant among all descent routes. Here, its necessity is elucidated.

First, we conclude from our analysis that it is rare for parcels to be transported within mid-latitudes from high to low altitudes while maintaining high concentrations of ^{7}Be included in high-altitude parcels (Kownacka, 2002; Land and Feichter, 2003): in this route, as mentioned in Sect. 4.2.2, parcels at high altitudes necessarily mix with those at low altitudes. This means that ^{7}Be concentrations inevitably decrease; therefore, the mid-latitude route is not a typical one, as observational events of high concentrations of ^{7}Be indicate. Therefore, for parcels to arrive at the near-surface level (about 2000–3000 m) at mid-latitudes while conserving their potential temperature, i.e., maintaining high concentrations of ^{7}Be, their starting area should be high latitudes, where the potential temperature is nearly the same as that in the arrival area. Moreover, owing to its long-distance transport, large-scale disturbances are always included. Thus, parcels always ride on the northerly wind associated with developed troughs.

In the high-latitude route, the altitudes of the parcels are generally lowered by tropopause folding, and the parcels are then transported to mid-latitudes. This process is also inevitable and is explained below.

Figure 19 shows the meridional inclination of each potential temperature with reference to the monthly-mean potential temperature at 8000 and 10 000 m at 70° N. The inclination of the potential temperature in each month is not markedly different with reference to the 8000 m potential temperature, although the potential temperature itself is different. That is, no particular month is easier than the other for effective parcel descent from high to low altitudes during the movement from high to mid-latitudes. In contrast, a significant difference is noted between the inclinations of the two reference altitudes of 8000 and 10 000 m. That is, isentropic surfaces for the 8000 m reference have large inclinations, whereas those for the 10 000 m reference have little inclinations.

On the basis of these results, the following conclusions are drawn. First, when parcels are transported from high to mid-latitudes at altitudes of more than 10 000 m, the height changes little. In contrast, when the starting altitudes are near 8000 m, the parcel height decreases dramatically during the movement to mid-latitudes. Thus, for parcels in the stratosphere to effectively reach low altitudes at mid-latitudes, the parcel height must diminish to less than 10 000 m. Furthermore, a larger decrease is related to more effective access to the surface. For this reason, a potential path for parcel descent is with tropopause folding at the initial stage.

5.2 Reason for frequent high-concentration days in spring

In this subsection, we clarify the reason for the large number of high-concentration days of ^{7}Be at Fukuoka in spring. Three possibilities are given considering the descent route: the frequency of tropopause folding at high latitudes, disturbances that transport parcels southward from high latitudes, and near-surface disturbances in the transport of parcels to the surface are different between spring and other seasons. Of course, high-concentration days of ^{7}Be appear easily when frequencies of tropopause folding are high, disturbances transporting the parcels southward are strong, and parcels are effectively transported to the surface by near-surface disturbances. The difference in the meridional inclination of isentropic surfaces in the troposphere is one possibility. However, as shown in the previous subsection, this difference is small enough to be excluded from the possibilities. Then, these three are examined. The data used for these analyses are the 1.25°-grid isentropic analysis data for frequencies of tropopause folding and disturbances transporting parcels southward in addition to the model-grid data for near-surface disturbances.

The climatological tropopause folding was examined by Sprenger et al. (2003) (see also Añel et al. 2008). However, their definition seems to cover exclusively folding with bending, but does not cover folding with straightly trailing down. Therefore, we make our own definition, examining tropopause folding. The definition is the state at which the PV surface of 3 PVU trails down to less than ~~6000m~~6000 m, although this definition may be a bit exclusive, and it may apply to cases with no precise tropopause folding. Figure 20 shows the seasonal difference in the frequencies of tropopause folding at 30° W–120° E, hereafter referred to as the Eurasian region. This region nearly corresponds to the starting region of the parcels, as shown in Fig. 3a. Figure 20 shows that the tropopause folds are

frequent at high latitudes in spring and at 40–50° N in winter. The frequencies are generally slightly higher in spring than in winter. For our purposes, however, we consider that these two seasons show no significant differences. Low frequencies in summer and autumn can explain the lower number of high-concentration days in these two seasons. Needless to say, a more detailed analysis of tropopause folding in high latitudes is necessary, because its definition adopted in this study is rough.

Next, disturbances transporting parcels southward are examined. Because parcels are transported by the northerly wind at the rear side of troughs, the strength of the northerly is examined such that the 2–8-day period component of the meridional wind is extracted, and its variance is compared. The variances in winter and spring among the four seasons are shown in Fig. 21. Although the variance is larger in winter than in spring in the Pacific and Atlantic regions, it is larger in spring than in winter in the Eurasian region in question. In winter, we consider that disturbances in that region are weak because the connection is weak from the storm track region in the Atlantic to the polar frontal jet in the Eurasian region, and disturbances in the Atlantic are connected to the strong-wind region in the Mediterranean. In contrast, in spring, owing to the weak wind in the Mediterranean, the polar frontal jet is connected to the storm track region in the Atlantic; thus, the disturbances are considered to be strong in the polar frontal jet. For the other seasons, the variance in autumn shows almost the same feature as that in spring, and the variance in summer is very small (not shown).

Finally, the differences in near-surface disturbances are investigated. The working hypothesis is that near-surface disturbances and their associated wind systems show marked characteristics between seasons, and some wind systems match and other systems mismatch parcels coming to Fukuoka by subsidence from low altitudes at mid-latitudes. For example, in winter, parcels are usually transported to Japan from the north within low altitudes owing to the dominance of the northerly winter monsoon, resulting in a mismatch of the wind system with the descent routes clarified thus far. Then, we examined the differences in backward trajectories between January 2011, when no high-concentration events occurred, and April of the same year. Backward trajectories were calculated for 31 and 30 times starting from 00:00 UTC on all days in January and April, respectively.

Figure 22 shows the results. The backward trajectories drastically differ between January and April: all trajectories in January move northward, advancing to higher latitudes while maintaining relatively low altitudes, whereas those in April show both northward and southward movements with many ascending to relatively high altitudes. Of course, eastward and westward movements also exist (not shown). This characteristic of movements in various directions in April is consistent with that shown in Fig. 5. These features in January and April are confirmed to be similar in other years.

Similar calculations were conducted in July and October. The trajectories in October are similar to those in April. In July, many trajectories move southward, although some move in other directions. In addition, many trajectories remain within very low altitudes of less than 2000 m for four days.

From the above, the reason for the frequent high-concentration days in spring is clear: in spring, tropopause folds are frequent at high latitudes, disturbances transporting parcels southward are

strong, and near-surface disturbances lowering parcels to the surface are ubiquitous. On the other hand, some of these conditions are unfavorable in the other three seasons. In winter, although tropopause folds are frequent, the wind transporting parcels southward is not as strong, and in particular, near-surface disturbances transporting them to the surface do not exist in general. In autumn, although the last two conditions are favorable, tropopause folds are not frequent. In summer, all three conditions are unfavorable. As a result, high-concentration events of ^{7}Be are virtually absent.

6 Conclusions and future perspective

By using high concentrations of ^{7}Be as an indicator, fast descent routes from within or near the stratosphere to Earth's surface, with the study site being in Fukuoka, Japan, were elucidated. Here, "fast" means "within 10 days".

The majority of descent routes are from high latitudes and follow a particular sequence, as shown in Fig. 23: first, a descent associated with tropopause folding occurs, followed by southward movement with slow descent by the northerly wind at the rear side of a strong trough. Because this motion is along isentropic surfaces, air parcels descend while nearly conserving their potential temperature. In this extension, a strong descent associated with a sharp drop in isentropic-surface height occurs at the southern edge of the trough. This process involves irreversible phenomena such as filamentation and cutoff of potential vorticity. Therefore, descending parcels migrate at low altitudes without the turnaround along the southern edge of a trough and subsequent northward movement with slow ascent. Finally, by meeting near-surface disturbances to transport parcels from low altitudes to Earth's surface, the parcels are transported to the surface. These disturbances ~~occur in~~ have no specific form but various forms. ~~Figure 23 shows a schematic of this mechanism.~~ The daily variation of the atmospheric boundary layer (ABL) is important for the air parcels on the trajectories intruding into the ABL. That is, the air parcels above the ABL are easily taken into the ABL due to the development of the mixed layer during daytime, while it is difficult for them to enter the ABL during nighttime.

In some cases, parcels descend directly from high altitudes within mid-latitudes. In such cases, the potential temperature is not conserved; instead, it decreases. This result occurs because the potential temperature is high in these regions, and large descent never occurs while conserving the potential temperature. Thus, a decrease in potential temperature is inevitable for large descents. For this to occur, a diffluent-wind field on isentropic surfaces is necessary, where some part of the flow moves northward, and the other part moves southward with descent. When these descending parcels push low isentropic surfaces, their potential temperature decreases upon mixing with parcels having lower potential temperature at lower altitudes. Then, by the repetition of this process, the height of the parcels decreases drastically. The route from low altitudes to the surface is the same as in the high-latitude route as mentioned above.

We clarified the necessity that the high-latitude route is dominant. In the mid-latitude route, the mixing between parcels at high and relatively low altitudes is inevitable; that is, the high concentrations of ^{7}Be in high-altitude parcels are difficult to maintain. Therefore, for parcels to arrive at low altitudes in the mid-latitudes while maintaining high concentrations of ^{7}Be, i.e., conserving the potential temperature, their starting area should be high altitudes at high latitudes, where the potential temperature is nearly the same as that in the arrival area. In addition, we revealed the reason for the mandatory initial descent; when parcels in the stratosphere start to move to mid-latitudes, descent never occurs. In contrast, for descent to be effective, it is necessary that parcels must already be lowered from the stratosphere to the troposphere at high latitudes before moving to mid-latitudes.

Many high-concentration events of ^{7}Be occur in spring because in this season, tropopause folds are frequent at high latitudes, disturbances transporting parcels southward are strong, and near-surface disturbances lowering them to the surface are ubiquitous. On the other hand, because some of these conditions are unfavorable in the other three seasons, high-concentration events of ^{7}Be are not frequent. In particular, they are virtually absent in summer.

Finally, we present a view of future work following the present study. This study examined fast descent routes to a specific location, i.e., Fukuoka, Japan. However, by extending the present results, we can examine fast descent routes to other locations; we believe that the majority of them are from regions in which tropopause folds are frequent. As confirmed in relation to Fig. 20, such regions include the northeastern part of the Asian continent and the northern and northeastern parts of North America in spring, in addition to the northern part of North America and storm track regions in the Pacific and Atlantic in winter (not shown). Then, if forward trajectories are traced from these regions with starting times at which tropopause folding occurs, some trajectories may arrive at the surface. From these calculations, many fast descent routes will be revealed.

Furthermore, it is interesting to consider the material and chemical differences in the air in regions of fast descent routes from those of general tropospheric air. We can easily predict elevated ozone concentrations and low specific humidity; however, other characteristics are possible. Therefore, several new research topics such as chemical reactions in the air will be discussed in future.

Acknowledgements. We would like to thank S. Miyahara for many useful comments in the development of this work. Thanks are extended to the three anonymous reviewers for many valuable and constructive comments. In particular, one reviewer recommended an analysis of the difference in the behaviour of the air parcels on the trajectories between daytime and nighttime in the atmospheric boundary layer. These comments led to substantial improvements of the paper. The GFD-DENNOU Libraries and GrADS were used for producing the figures.

References

Ambrose, J. L., Reidmiller, D. R., Jaffe, D. A., Causes of high O_3 in the lower free troposphere over the Pacific Northwest as observed at the Mt. Bachelor Observatory. Atmos. Environ. 45, 5302–5315, 2011.

Añel, J. A., Antuña, J. C., de la Torre, L., Castanheira, J. M., and Gimeno, L., Climatological features of global multiple tropopause events, J. Geophys. Res., 113, D00B08, doi:10.1029/2007JD009697, 2008.

Bezuglov, M. V., Malyshevsky, V. S., Fomin, G. V., Torgovkin, A. V., Shramenko, B. I., and Malykhina, T. V.: Photonuclear production of cosmogenic beryllium-7 in the terrestrial atmosphere, Phys. Rev. C, 86, 024609, doi:10.1103/PhysRevC.86.024609, 2012.

Bracci, A., Cristofanelli, P., Sprenger, M., Bonafe, U., Calzolari, F., Duchi, R., Laj, P., Marinoni, A., Roccato, F., E. Vuillermoz, E., and Bonasoni, P., Transport of stratospheric air masses to the Nepal Climate Observatory-Pyramid (Himalaya; 5079 m MSL): A synoptic-scale investigation, J. Appl. Meteor. Climatology, 51, 1489–1507, 2012.

Buraeva, E. A., Davydov, M. G., Zorina, L. V., Malyshevskii, V. S., and Stasov, V. V.: Content of cosmogenic ^{7}Be in the air layer at the ground at temperate latitudes, Atom. Energy, 102, 463–468, 2007.

Chen,~~X.~~ X., Añel, J. A., Su, Z., de la Torre, L., ~~Ma~~Kelder, H., van Peet, J., and Ma, Y., The deep atmospheric boundary layer and its significance to the stratosphere and troposphere exchange over the Tibetan Plateau. PLoS ONE, 8, ~~Y. M.~~ e56 909, doi:10.1371/journal.pone.0056909, 2013.

Chen, X., Ma, Y., Kelder, H., Su, Z., Yang, K., On the behavior of the tropopause folding events over the Tibetan Plateau~~.~~, Atmos. Chem. Phys. 11, 5113–5122. 2011.

Chen, X., Škerlak, B., Rotach, M. W., Añel, J. A., Su, Z., Ma, Y., Li, M., Reasons for the extremely high-ranging planetary boundary layer over the western Tibetan Plateau in winter, J. Atmos. Sci.,doi:10.1175/JAS-D-15-0148.1, in press, 2016.

Cristofanelli, P., Bonasoni, P., Collins, W., Feichter, J., Forster, C., James, P., Kentarchos, A., Kubik, P. W., Land, C., Meloen, J., Roelofs, G. J., Siegmund, P., Sprenger, M., Schnabel, C., Stohl, A., Tobler, L., Tositti, L., Trickl, T., and Zanis, P.: Stratosphere-to-troposphere transport: a model and method evaluation, J. Geophys. Res., 108, 8525, doi:10.1029/2002JD002600, 2003.

Cristofanelli, P., Bonasoni, P., Tositti, L., Bonafé, U., Calzolari, F., Evangelisti, F., Sandrini, S., Stohl, A., A 6-year analysis of stratospheric intrusions and their influence on ozone at Mt. Cimone (2165 m above sea level). J. Geophys. Res., 111, D03306, doi:10.1029/2005JD006553, 2006.

Cristofanelli, P., Bracci, A., Sprenger, M., Marinoni, A., Bonafe, U., Calzolari, F., Duchi, R., Laj, P., Pichon, J. M., Roccato, F., Venzac, H., Vuillermoz, E., and Bonasoni, P., Tropospheric ozone variations at the Nepal Climate Observatory-Pyramid (Himalayas, ~~5079ma~~5079m a.s.l.) and influence of deep stratospheric intrusion events, Atmos. Chem. Phys., 10, 6537–6549, 2010.

Eisele, H., Scheel, H. E., Sladkovic, R., and Trickl, T., High-resolution lidar measurements of stratosphere-troposphere exchange, J. Atmos. Sci., 56, 319–330, 1999.

Elbern, H., Kowol, J., Sladkovic, R., and Ebel, A.: Deep stratospheric intrusions: a statistical assessment with model guided analysis, Atmos. Environ., 31, 3207–3226, 1997.

Feely, H. W., Larsen, R. J., and Sanderson, C. G.: Factors that cause seasonal variations in beryllium-7 concentrations in surface air, J. Environ. Radioactiv., 9, 223–249, 1989.

Gerasopoulos, E., Zanis, P., Stohl, A., Zerefos, C. S., Papastefanou, C., Ringer, W., Tobler, L., Hübener, S., Gäggeler, H. W., Kanter, H. J., Tositti, L., and Sandrini, S.: A climatology of ^{7}Be at four high-altitude stations at the Alps and the Northern Apennines, Atmos. Environ., 35, 6347–6360, 2001.

Holton, J. R., Haynes, P. H., McIntyre, M. E., Douglass, A. R., Rood, R. B., and Pfister, L.: Stratosphere-troposphere exchange, Rev. Geophys., 33, 403–440, 1995.

Hoskins, B. J., McIntyre, M. E., and Robertson, A. W.: On the use and significance of isentropic potential vorticity maps, Q. J. Roy. Meteor. Soc., 111, 877–946, 1985.

James, P., Stohl, A., Forster, C., Eckhardt, S., Seibert, P., and Frank, A.: A 15-year climatology of stratosphere-troposphere exchange with a Lagrangian particle dispersion model: 1. Methodology and validation, J. Geophys. Res., 108, 8519, doi:10.1029/2002JD002637, 2003a.

James, P., Stohl, A., Forster, C., Eckhardt, S., Seibert, P., and Frank, A.: A 15-year climatology of stratosphere-troposphere exchange with a Lagrangian particle dispersion model: 2. Mean climate and seasonal variability, J. Geophys. Res., 108, 8522, doi:10.1029/2002JD002639, 2003b.

Jordan, C. E., Dibb, J. E., and Finkel, R. C.: ^{10}Be/^{7}Be tracer of atmospheric transport and stratosphere-troposphere exchange, J. Geophys. Res., 108, 4234, doi:10.1029/2002JD002395, 2003.

Kikuchi, S., Sakurai, H., Gunji, S., and Tokanai, F.: Temporal variation of ^{7}Be concentrations in atmosphere for 8 y from 2000 at Yamagata, Japan: solar influence on the ^{7}Be time series, J. Environ. Radioactiv., 100, 515–521, 2009.

Kobayashi, S., Ota, Y., Harada, Y., Ebita, A., Moriya, M., Onoda, H., Onogi, K., Kamahori, H., Kobayashi, C., Endo, H., Miyaoka, K., and Takahashi, K.: The JRA-55 reanalysis: General specifications and basic characteristics, J. Meteorol. Soc. Jpn., 93, 5–48, 2015.

Kownacka, L., Vertical distributions of beryllium-7 and lead-210 in the tropospheric and lower stratospheric air, NUKLEONIKA, 47, 79–82, 2002.

Land, C., and Feichter, J., Stratosphere-troposphere exchange in a changing climate simulated with the general circulation model MAECHAM4, J. Geophys. Res., 108, 8523, doi:10.1029/2002JD002543, 2003.

Langford, A. O., Brioude, J., Cooper, O. R., Senff, C. J., Alvarez II, R. J.,Hardesty, R. M., Johnson, B. J., and Oltmans, S. J., Stratospheric influence on surface ozone in the Los Angeles area during late spring and early summer of 2010, J. Geophys. Res., 117, D00V06, doi:10.1029/2011JD016766, 2012.

Langford, A. O., Senff, C. J., Alvarez, R. J., Brioude, J., Cooper, O. R., Holloway, J. S., Lin, M. Y., Marchbanks, R. D., Pierce, R. B., Sandberg, S. P., Weickmann, A. M., and Williams, E. J.: An overview of the 2013 Las Vegas Ozone Study (LVOS): impact of stratospheric intrusions and long-range transport on surface air quality, Atmos. Environ., 109, 305–322, doi:10.1016/j.atmosenv.2014.08.040, 2015.

Lefohn, A. S., Wernli, H., Shadwick, D., Oltmans, S. J., Shapiro, M., Quantifying the importance of stratospheric-tropospheric transport on surface ozone concentrations at high- and low-elevation monitoring sites in the United States. Atmos. Environ. 62, 646–656, 2012.

Lin, M., Fiore, A. M., Cooper, O. R., Horowitz, L. W., Langford, A. O., Levy, H., Johnson, B. J., Naik, V., Oltmans, S. J., and Senff, C. J.: Springtime high surface ozone events over the western United States: quantifying the role of stratospheric intrusions, J. Geophys. Res., 117, D00V22, doi:10.1029/2012JD018151, 2012.

Lin, M., Fiore, A. M., Horowitz, L. W., Langford, A. O., Oltmans, S. J., Tarasick, D., and Rieder, H. E., Climate variability modulates western US ozone air quality in spring via deep stratospheric intrusions, Nature Commun., 6:7105, doi:10.1038/ncomms8105, 2015.

Ma, J., Lin, W. L., Zheng, X. D., Xu, X. B., Li, Z., and Yang, L. L., Influence of air mass downward transport on the variability of surface ozone at Xianggelila Regional Atmosphere Background Station, southwest China, Atmos. Chem. Phys., 14, 5311–5325, 2014.

Machta, L., 1957: Discussion of meteorological factors and fallout distribution, U.S. Weather Bureau, 11 pp.

Masarik, J., and Beer, J., Simulation of particle fluxes and cosmogenic nuclide production in the Earth's atmosphere, J. Geophys. Res., 104, 12 099-12 111, 1999.

Megumi, K., Matsunami, T., Ito, N., Kiyoda, S., Mizohata, A., and Asano, T.: Factors, especially sunspot number, causing variations in surface air concentrations and depositions of ^{7}Be in Osaka, Japan, Geophys. Res. Lett., 27, 361–364, 2000.

Nagai, H., Tada, W., and Kobayashi, T.: Production rates of ^{7}Be and ^{10}Be in the atmosphere, Nucl. Instrum. Methods, 172, 796–801, 2000.

Narazaki, Y. and Fujitaka, K.: Cosmogenic ^{7}Be: atmospheric concentration and deposition in Japan, Japanese J. Health Phy., 44, 95–105, 2009.

Nieto, R., Sprenger, M., Wernli, H., Trigo, R. M., and ~~Gimenoa~~Gimeno, L., Identification and climatology of cut-off lows near the tropopause, Trend. Direct. Climate Res., Ann. N.Y. Acad. Sci., 1146, 256–290, 2008.

Ojha, N., Najaa, M., Sarangi, T., Kumar, R., Bhardwaj P, Lal, S., Venkataramani , S., Sagar, R., Kumar, A., Chandola, H. C., On the processes influencing the vertical distribution of ozone over the central Himalayas: Analysis of yearlong ozonesonde observations, Atmos. Environ., 88, 201–211, 2014.

Oltmans, S. J., Levy, II. H., Seasonal cycle of surface ozone over the western North Atlantic. Nature, 358, 392–394, 1992.

Raisbeck, G. M., Yiou, F., Fruneau, M., Loiseaux, J. M., Lieuvin, M., and Ravel, J. C.: Cosmogenic ^{10}Be/^{7}Be as a probe of atmospheric transport processes, Geophys. Res. Lett., 8, 1015–1018, 1981.

Reed, R. J., and F. Sanders, An investigation of the development of a mid-tropospheric frontal zone and its associated vorticity field, J. Meteor., 10, 338-349, 1953.

Škerlak, B., Sprenger, M., and Wernli, H.: A global climatology of stratosphere–troposphere exchange using the ERA-Interim data set from 1979 to 2011, Atmos. Chem. Phys., 14, 913–937, doi:10.5194/acp-14-913-2014, 2014.

Sprenger, M. and Wernli, H.: A Northern Hemisphere climatology of cross-tropopause exchange for the ERA15 time period (1979–1993), J. Geophys. Res., 108, D128521, doi:10.1029/2002JD002636, 2003.

Sprenger, M., Croci Maspoli, M., and Wernli, H.: Tropopause folds and cross-tropopause transport: a global investigation based upon ECMWF analyses for the time period March 2000 to February 2001, J. Geophys. Res., 108, 8518, doi:10.1029/2002JD002587, 2003.

Stohl, A., Bonasoni, P., Cristofanelli, P., Collins, W., Feichter, J., Frank, A., Forster, C., Gerasopoulos, E., Gäggeler, H., James, P., Kentarchos, T., Kromp-Kolb, H., Krüger, B., Land, C., Meloen, J., Papayannis, A., Priller, A., Seibert, P., Sprenger, M., Roelofs, G. J., Scheel, H. E., Schnabel, C., Siegmund, P., Tobler, L., Trickl, T., Wernli, H., Wirth, V., Zanis, P., and Zerefos, C.: Stratosphere-troposphere exchange: a review, and what we have learned from STACCATO, J. Geophys. Res., 108, 8516, doi:10.1029/2002JD002490, 2003.

Stohl, A., Spichtinger-Rakowsky, N., Bonasoni, P., Feldmann, H., Memmesheimer, M., Scheel, H. E., Trickl, T., Hubener, S., Ringer, W., and Mandl, M.: The influence of stratospheric intrusions on Alpine ozone concentrations. Atmos. Environ., 34, 1323–1354, 2000.

Tositti, L., Brattich, E, Cinelli, G., Baldacci, D., 12 years of ^{7}Be and ^{210}Pb in Mt. Cimone, and their correlation with meteorological parameters, Atmos. Environ., 87, 108–122, 2014.

Trickl, T., Feldmann, H., Kanter, H. J., Scheel, H. E., Sprenger, M., Stohl, A., and Wernli, H., Forecasted deep stratospheric intrusions over Central Europe: case studies and climatologies, Atmos. Chem. Phys., 10, 499–524, 2010.

Trickl, T., Vogelmann, H., Giehl, H., Scheel, H. E., Sprenger, M., and Stohl, A., How stratospheric are deep stratospheric intrusions? Atmos. Chem. Phys., 14, 9941–9961, 2014.

Tsutsumi, Y., Igarashi, Y., Zaizen, Y., and Makino, Y.: Case studies of tropospheric ozone events observed at the summit of Mount Fuji, J. Geophys. Res., 103, 16935–16951, 1998.

US Environmental Protection Agency (US EPA): Air Quality Criteria for Ozone and Related Photochemical Oxidants (2006 Final), EPA/600/R-05/004aF-cF, US Environ. Prot. Agency, Washington, D.C., USA, 821 pp., 2006.

Usoskin, I. G. and Kovaltsov, G. A.: Production of cosmogenic ^{7}Be isotope in the atmosphere: Full 3-D modeling, J. Geophys. Res., 113, D12107, doi:10.1029/2007JD009725, 2008.

Usoskin, I. G., Field, C. V., Schmidt, G. A., Leppänen, A.-P., Aldahan, A., Kovaltsov, G. A., Possnert, G., and Ungar, R. K.: Short-term production and synoptic influences on atmospheric ^{7}Be concentrations, J. Geophys. Res., 114, D06108, doi:10.1029/2008JD011333, 2009.

Wernli, H. and Bourqui, M.: A Lagrangian "1-year climatology" of (deep) cross-tropopause exchange in the extratropical Northern Hemisphere, J. Geophys. Res., 107, D24021, doi:10.1029/2001JD000812, 2002.

Yates, E. L., Iraci, L. T., Roby, M. C., Pierce, R. B., Johnson, M. S., Reddy, P. J., Tadić, J. M., Loewenstein, M., and Gore, W., Airborne observations and modeling of springtime stratosphere-to-troposphere transport over California, Atmos. Chem. Phys., 13, 12481–12494, 2013.

Zanis, P., Gerasopoulos, E., Priller, A., Schnabel, C., Stohl, A., Zerefos, C., Gäggeler, H. W., Tobler, L., Kubik, P. W., Kanter, H. J., Scheel, H. E., Luterbacher, J., and Berger, M.: An estimate of the impact of stratosphere-to-troposphere transport (STT) on the lower free tropospheric ozone over the Alps using ^{10}Be and ^{7}Be measurements, J. Geophys. Res., 108, 8520, doi:10.1029/2002JD002604, 2003.

Zheng, X.-D., Shen, C.-D., Wan, G.-J., Liu, K.-X., Tang, J., and Xu, X.-B.: ^{10}Be/^{7}Be implies the contribution of stratosphere-troposphere transport to the winter-spring surface O_3 variation observed on the Tibetan Plateau, Chinese Sci. Bull., 56, 84–88, 2011.

Table 1. Averages and standard deviations (SDs) of seasonal ^{7}Be concentrations in $\mathrm{mBq\,m^{-3}}$. "Days" denotes the total days of measurement. They are not integers because measurement times are not just 00:00 UTC. For instance, when measurement times are 00:00 UTC on some day and 01:00 UTC on the following day, $(1 + 1/24)$ days are added. The much lesser number of measurement days in SON than in the other seasons is attributed to the missing data owing to the earthquake-resistant retrofitting in 2014.

	Average	SD	Days
Total	5.20	2.19	2133.5
DJF	6.08	1.96	533.3
MAM	6.33	2.60	547.1
JJA	2.67	1.90	554.8
SON	5.83	2.22	498.3

Table 2. Numbers of seasonal and monthly high-concentration (HC) events of ^{7}Be and $\hat{z}_{\mathrm{a}}$ maximum events. Because the sampling intervals are not necessarily one day, the number of days is equal to or more than the number of events. The meanings of $\hat{z}_{\mathrm{a}}$ and $\hat{z}_1$ are referred to in the text. The bottom ~~three~~ four rows indicate classifications of the highest reached altitude in each event.

	DJF	March	April	May	JJA	SON	Total
HC events (number of days)	7 (9)	16 (18)	11 (11)	5 (11)	2 (2)	2 (4)	43 (56)
$\hat{z}_{\mathrm{a}}$ maximum events	7	15	12	9	1	2	47
$\hat{z}_1 \geq 10\,000\,\mathrm{m}$	1	1	1	1	1	0	5
$9000 \leq \hat{z}_1 < 10\,000\,\mathrm{m}$	0	2	3	2	1	1	9
$8000 \leq \hat{z}_1 < 9000\,\mathrm{m}$	2	6	4	6	0	1	19
$\hat{z}_1 < 8000\,\mathrm{m}$	4	6	4	0	0	0	14

Table 3. Time from the beginning of backward trajectories to the point of highest altitude (t_{a}), start time of maximum latitudinal movement per day (t_{m}), start time of the largest descent per day (t_{d}), and values of $t_{\mathrm{a}} - t_{\mathrm{m}}$ and $t_{\mathrm{m}} - t_{\mathrm{d}}$ with confidence intervals of 99 % are added. All the units are h. These values are shown for the 25 cases attaining the highest altitude north of 60° N.

Maximum altitude (t_{a})	Latitudinal movement (t_{m})	Descent (t_{d})	$t_{\mathrm{a}} - t_{\mathrm{m}}$	$t_{\mathrm{m}} - t_{\mathrm{d}}$
211.7	157.4	115.0	54.2 ± 27.5	42.4 ± 24.7

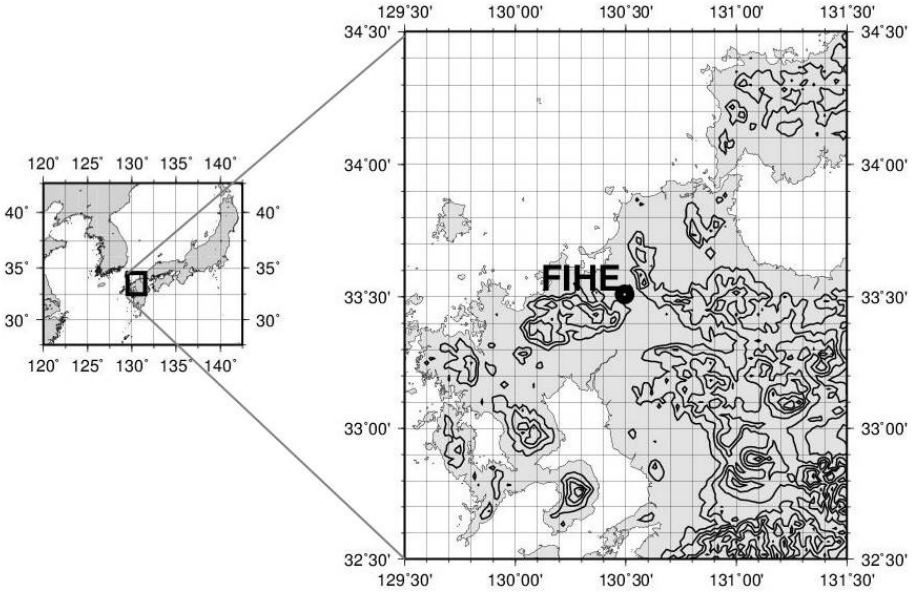

Figure 1. Map of the area near the Fukuoka Institute of Health and Environmental Sciences. Contours indicate altitude a.s.l. at intervals of 200 m.

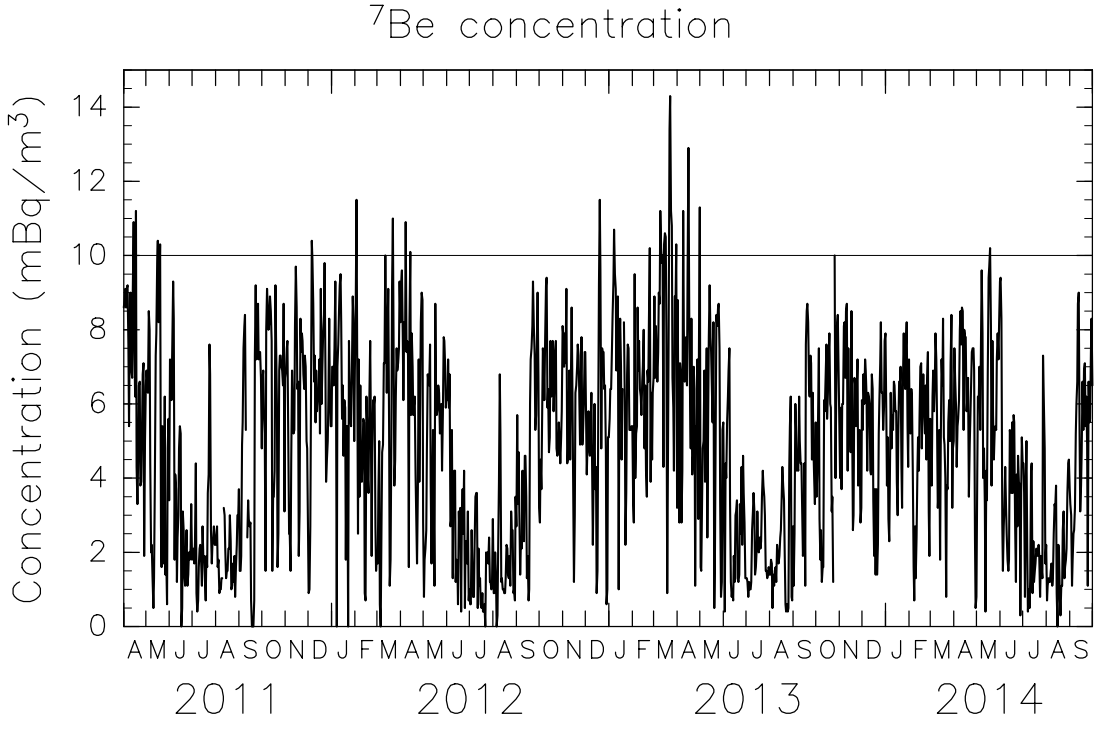

Figure 2. Time change of ^{7}Be concentrations from 1 April 2011 to 30 September 2014. The ordinate is ^{7}Be concentration (unit: mBq m^{-3}), and the abscissa is time. The horizontal line indicates 10 $\mathrm{mBq\,m^{-3}}$.

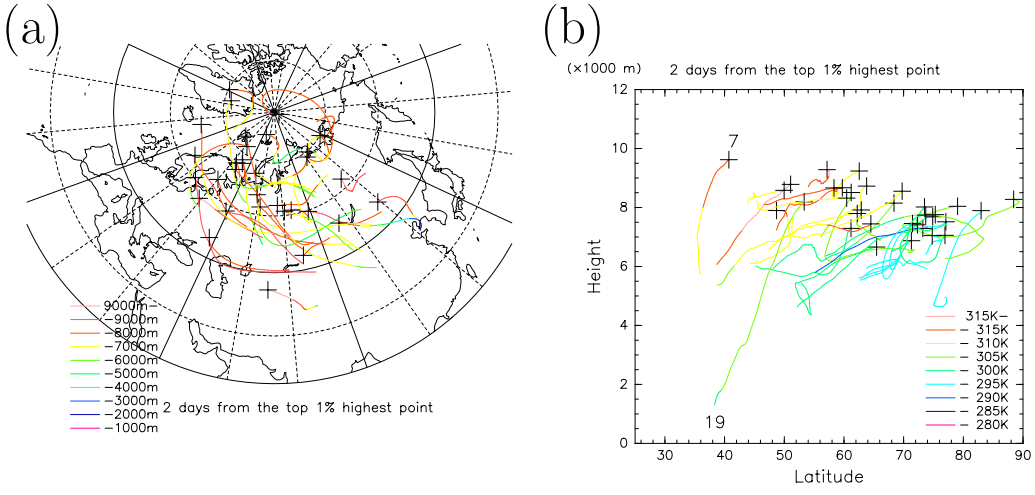

Figure 3. Top-1 % averaged trajectories for two days from their highest altitude. **(a)** Horizontal component of the trajectories and **(b)** trajectories in the latitude-vertical section for all 33 cases are shown. Colors indicate altitudes in panel **(a)** and potential temperature in panel **(b)**. The symbol + shows the position of the highest altitude of each top-1% averaged trajectory. The two numerals, 7 and 19, are the case numbers.

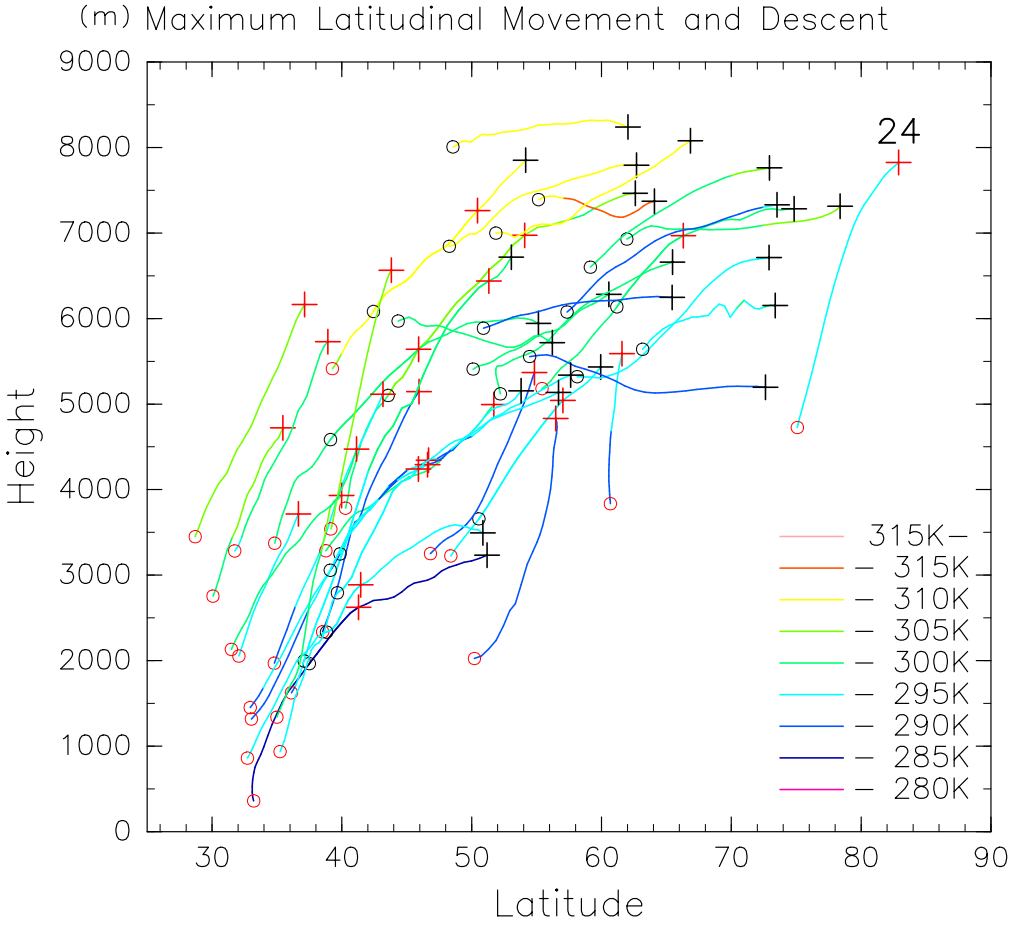

Figure 4. Paths showing the maximum latitudinal movement and maximum descent per day. The black (red) symbols of + and ○ indicate the starting and final positions, respectively, for the latitudinal movement (descent). The 25 cases showing the highest altitude north of 60° N are illustrated. The line color represents the potential temperature. The numeral (24) attached to the descent route shows the case number.

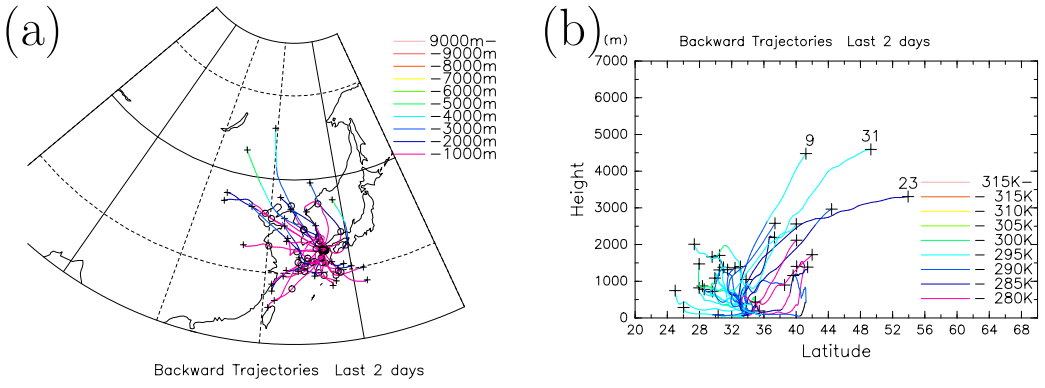

Figure 5. Top-1 % averaged trajectories for the last two days of travel. **(a)** Horizontal component of the trajectories and **(b)** trajectories in the latitude-vertical section for all 33 cases are shown. The colors are the same as those in Fig. 3. The + symbol indicates the position before two days of object times for analysis. The three numerals (9, 23, and 31) in panel **(b)** indicate the case numbers.

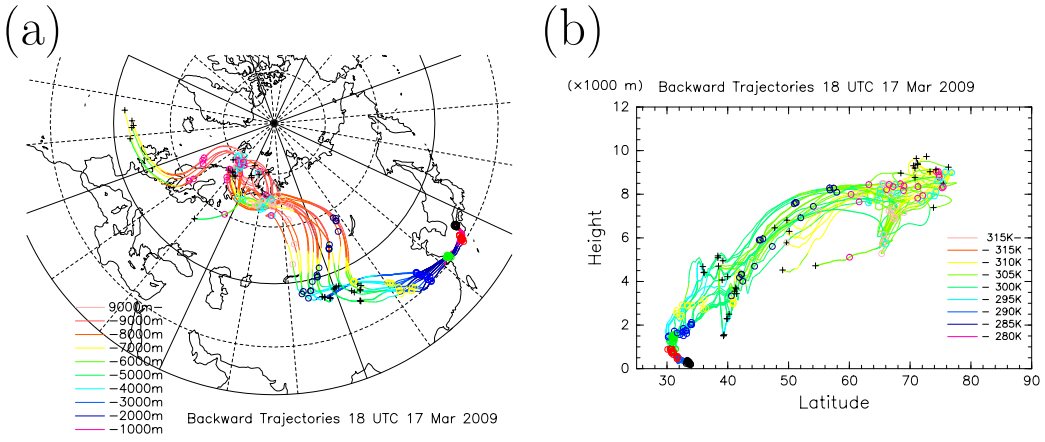

Figure 6. Backward trajectories starting at 18:00 UTC 17 March 2009 (case 1). **(a)** Horizontal component of the routes and **(b)** routes in the latitude-vertical section of the top-1 % trajectories (18 lines) and the top-25 % averaged trajectory (thick line) are shown. The colors are the same as those in Fig. 3. The ∘ symbol indicates positions at each 24 h interval, whereas the + symbol shows the fifth day and the last. The difference in days is represented by different colors.

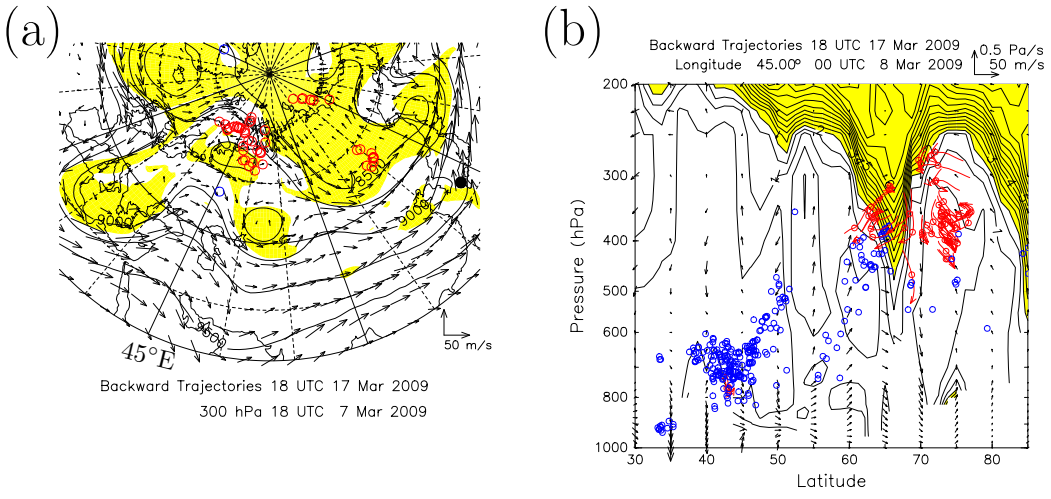

Figure 7. **(a)** 300 hPa surface map at 18:00 UTC 7 March and **(b)** the latitude-vertical section along 45° E at 00:00 UTC 8 March 2009. Height (contour; unit: m), wind (arrow), and PV (shading) are shown in panel **(a)**, and PV (contour and shading; unit: PVU) and meridional and vertical flow (arrow) are shown in panel **(b)**. The ordinate in panel **(b)** is pressure. Yellow areas in panels **(a, b)** indicate areas of more than 2 PVU. The symbol ○ represents positions of air parcels in backward trajectories for case 1, where all parcels are plotted within a height difference of 1000 m in panel **(a)** and within a longitudinal difference of 500 km in panel **(b)**. Red (blue) colors indicate parcels with more (less) than 2 PVU of PV. The black-filled circle in **(a)** indicates the position of Fukuoka. For parcels with more than 2 PVU or less than 350 hPa, their movements between 6 h before and after the present time are plotted by arrows in panel **(b)**. Flow speeds are indicated at the lower-right side in panel **(a)** and upper-right side in panel **(b)**.

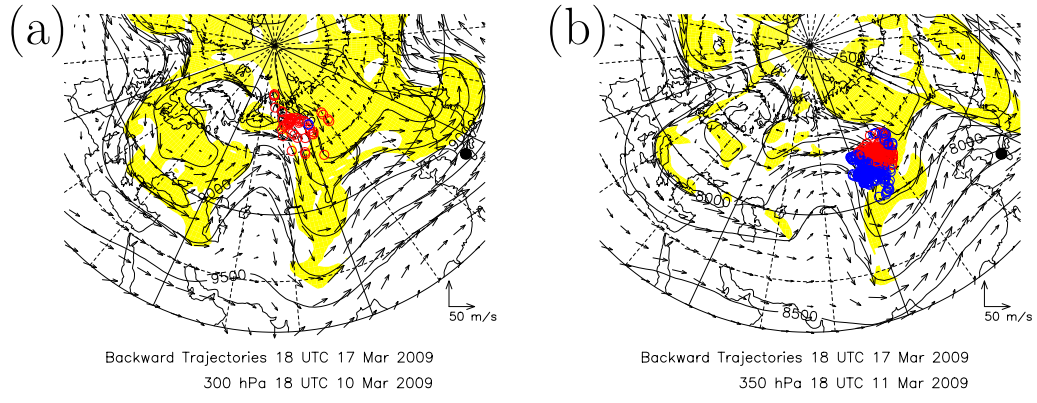

Figure 8. Same as Fig. 7a but for **(a)** 300 hPa surface at 18:00 UTC 10 March and **(b)** 350 hPa surface at 18:00 UTC 11 March 2009 in case 1.

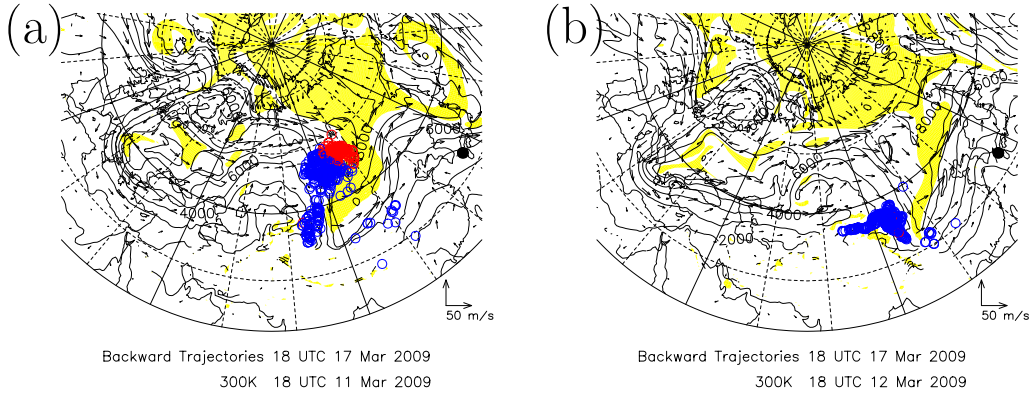

Figure 9. Same as Fig. 7a but for the 300 K isentropic surfaces at **(a)** 18:00 UTC 11 March, and **(b)** 18:00 UTC 12 March 2009 in case 1.

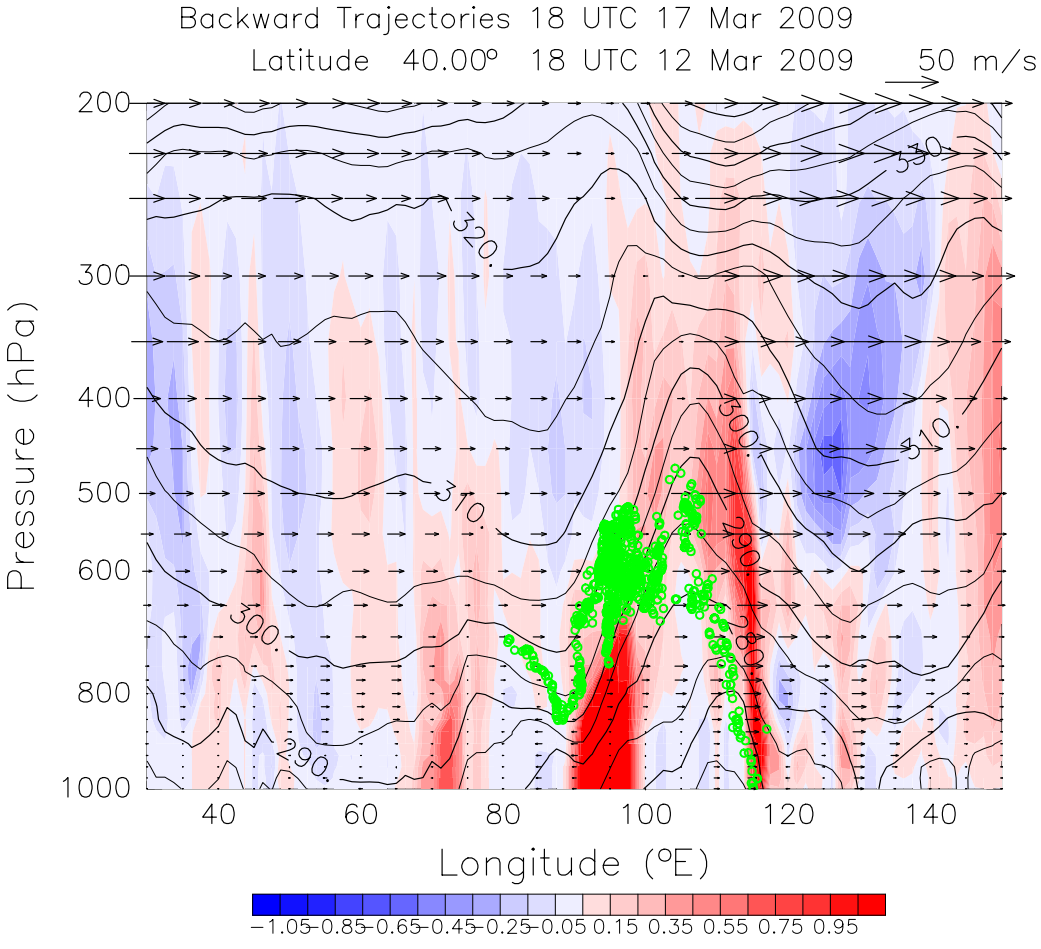

Figure 10. Longitude-vertical section along 40° N at 18:00 UTC 12 March 2009. Colors indicate vertical motions (unit: $\mathrm{Pa\,s^{-1}}$), and contours represent potential temperature (unit: K). Arrows show zonal wind, and their magnitudes are indicated at the upper-right side. Parcel positions within 500 km from 40° N in case 1 are plotted in green. The strong subsidence near 90° E may not be accurate because this area is a mountainous region.

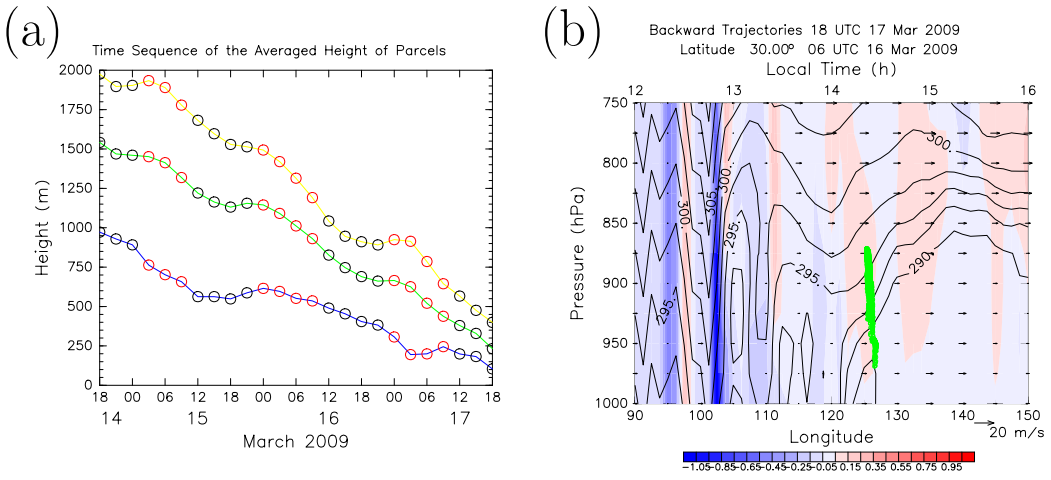

Figure 11. **(a)** Time change of the average heights of all the air parcels (green line), lowest-10 % parcels (blue line) and highest-10 % parcels (yellow line) on the trajectories for case 1. The ordinate is height, and the abscissa is time. The red and black circles indicate the average heights at daytime (8:00-20:00 Local Time) and nighttime (20:00-8:00 Local Time), respectively. **(b)** Same as Fig. 10 but for a small area along 30° N at 06:00 UTC 16 March 2009. In addition, the local time (h) is indicated in the upper axis.

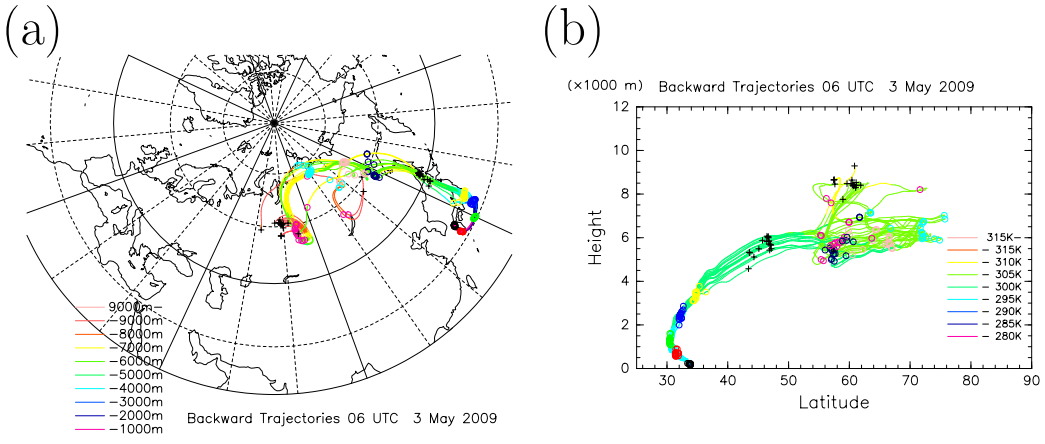

Figure 12. Same as Fig. 6 but for case 3 (starting time of 06:00 UTC 3 May 2009).

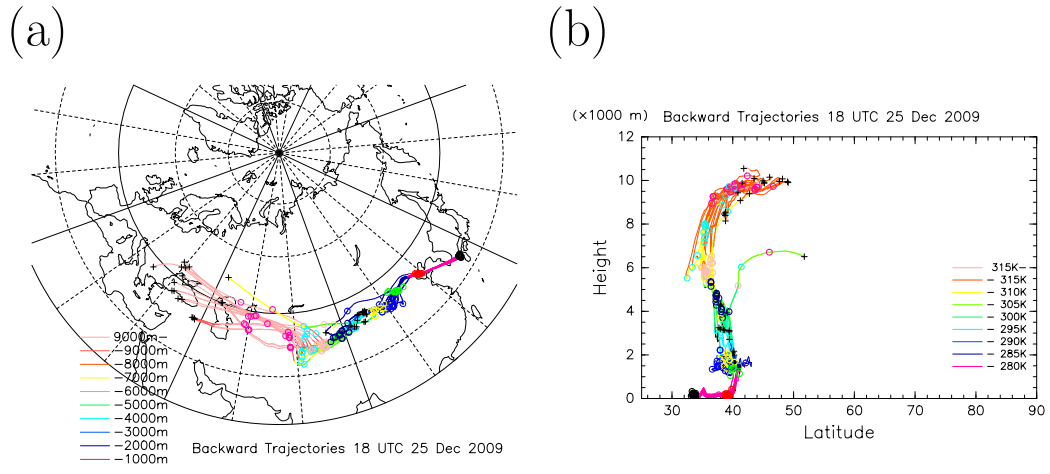

Figure 13. Same as Fig. 6 except for case 7 (starting time of 18:00 UTC 25 December 2009).

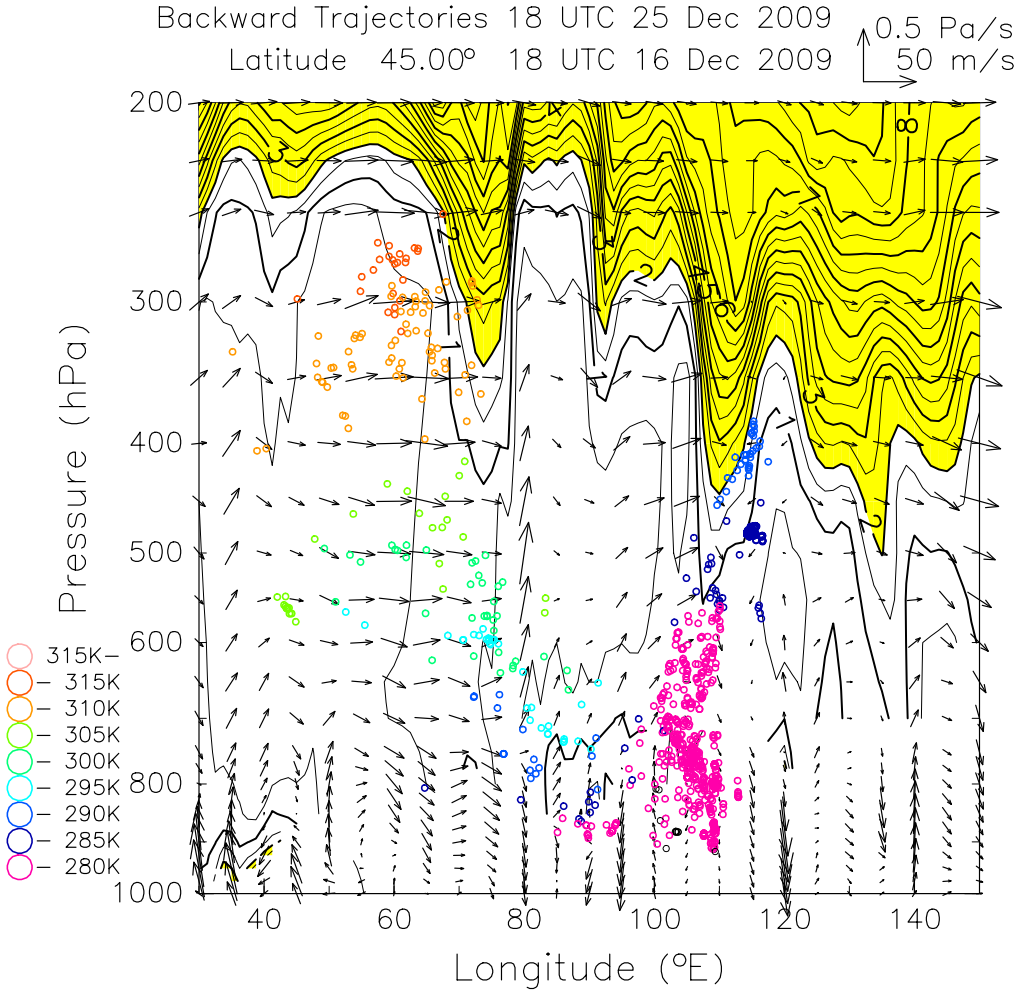

Figure 14. PV and parcel positions on backward trajectories in the longitude-vertical section along 45° N at 18:00 UTC 16 December 2009. Parcels within 500 km from 45° N are plotted with the potential temperature represented by color.

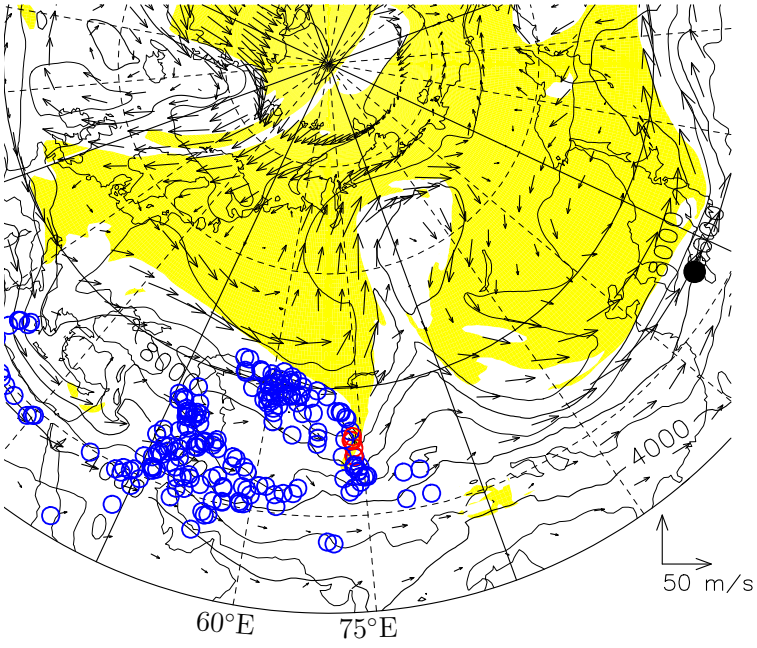

Figure 15. Same as Fig. 7a except for the 310 K isentropic surface at 18:00 UTC 16 December 2009.

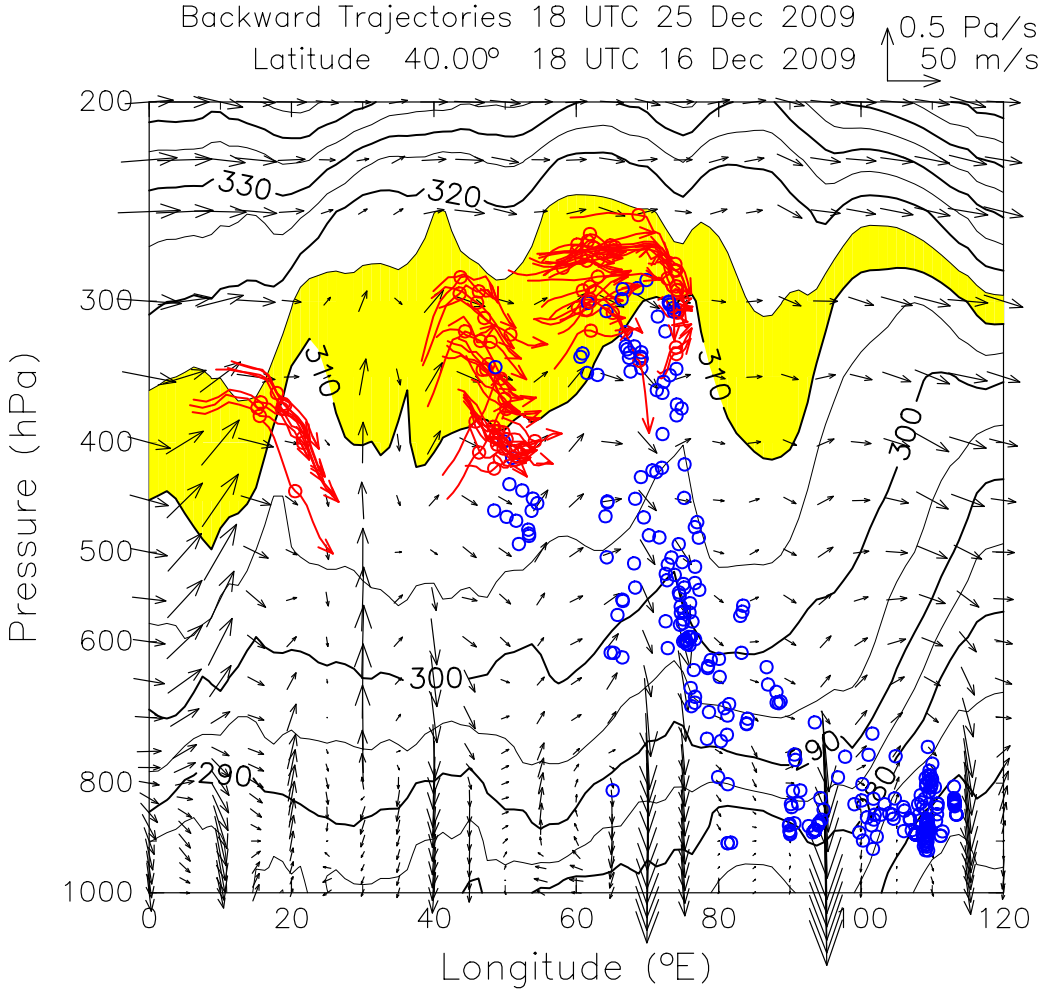

Figure 16. Potential temperature and parcel positions on backward trajectories in the longitude-vertical section along 40° N at 18:00 UTC 16 December 2009. Parcels with red (blue) color show potential temperature values of more (less) than 310 K. Movement between 6 h before and after the present time for red parcels is indicated by arrows.

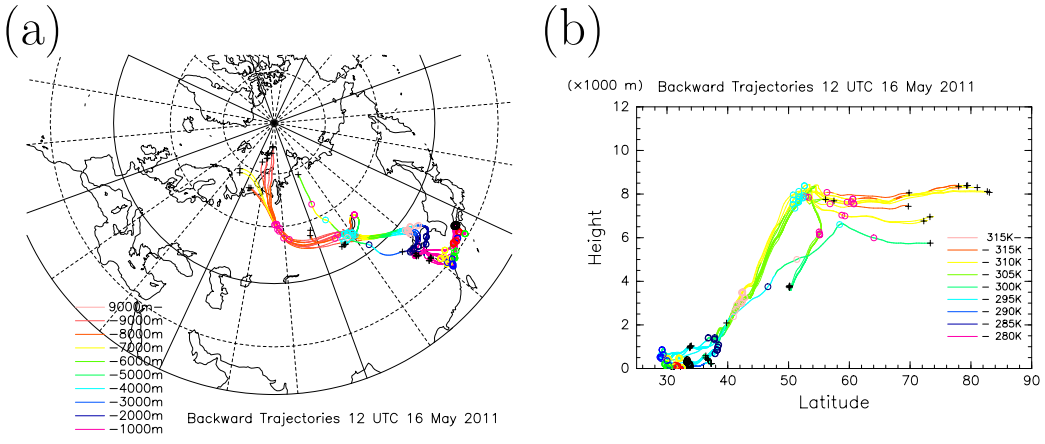

Figure 17. Same as Fig. 6 except for case 19 (starting time of 12:00 UTC 16 May 2011).

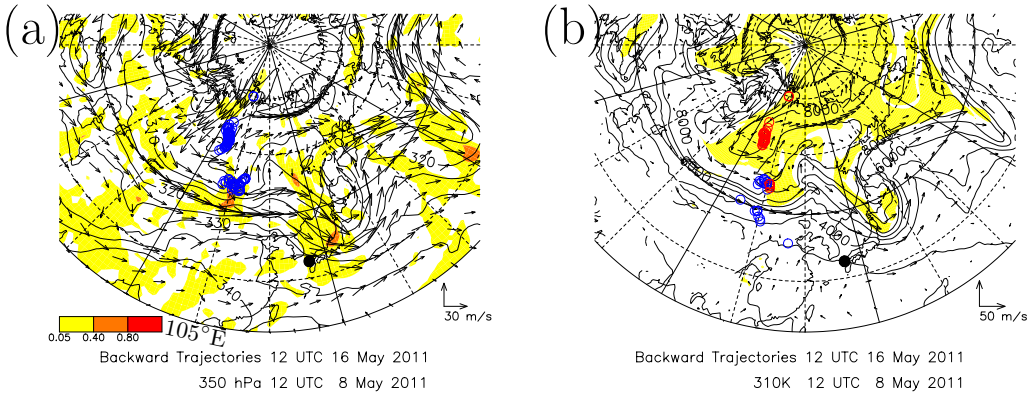

Figure 18. (a) Potential temperature (contour; unit: K), downward flow (shading; unit: Pa s^{-1}), and wind (arrows) on the 350 hPa level and **(b)** height (contour; unit: m) and wind (arrows) on the 300 K isentropic surface at 12:00 UTC 8 May 2011. Yellow colors indicate areas of more than 2 PVU in panel **(b)**. The parcel positions are shown within height differences of 1000 m.

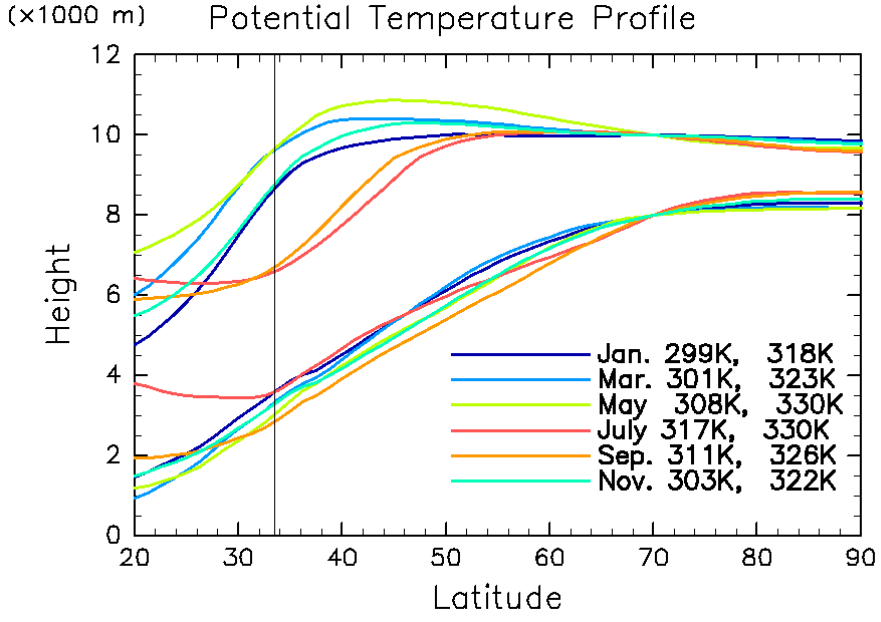

Figure 19. Meridional inclination of each potential temperature with reference to the monthly-mean potential temperature at 8000 and 10 000 m heights at 70° N. The potential temperature is shown at the right side of each month (left: 8000 m; right: 10 000 m). The averages between 30° W and 120° E are shown for only the odd months.

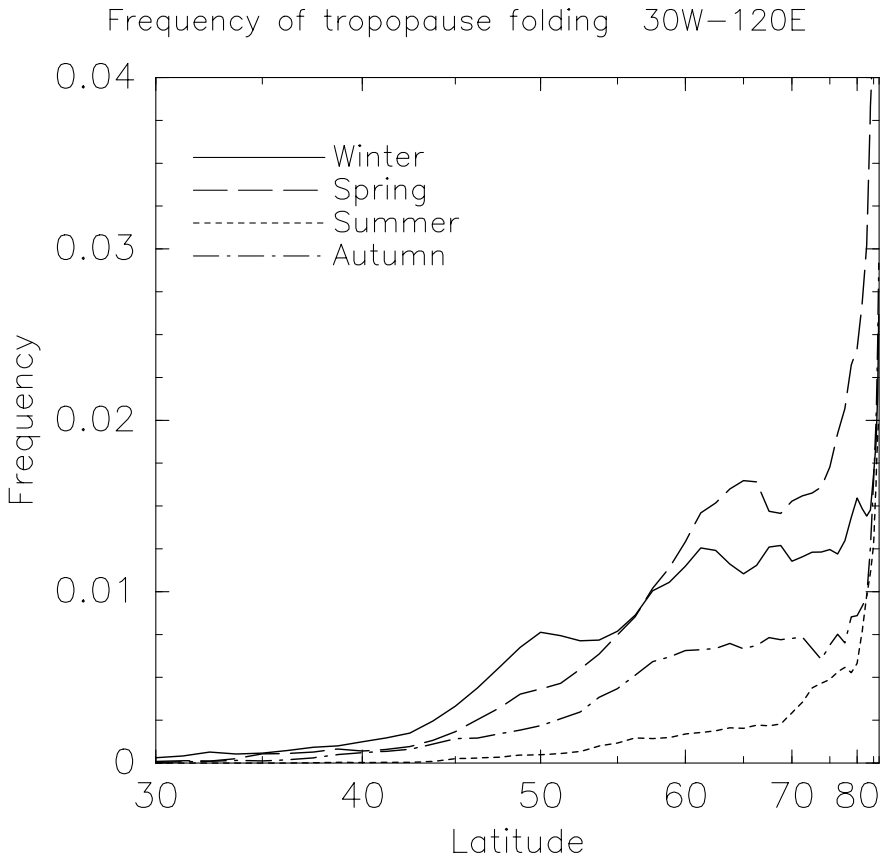

Figure 20. Seasonal frequencies of tropopause folding. The abscissa is the latitude elongated and contracted by the area factor. The frequencies are averaged between 30° W and 120° E.

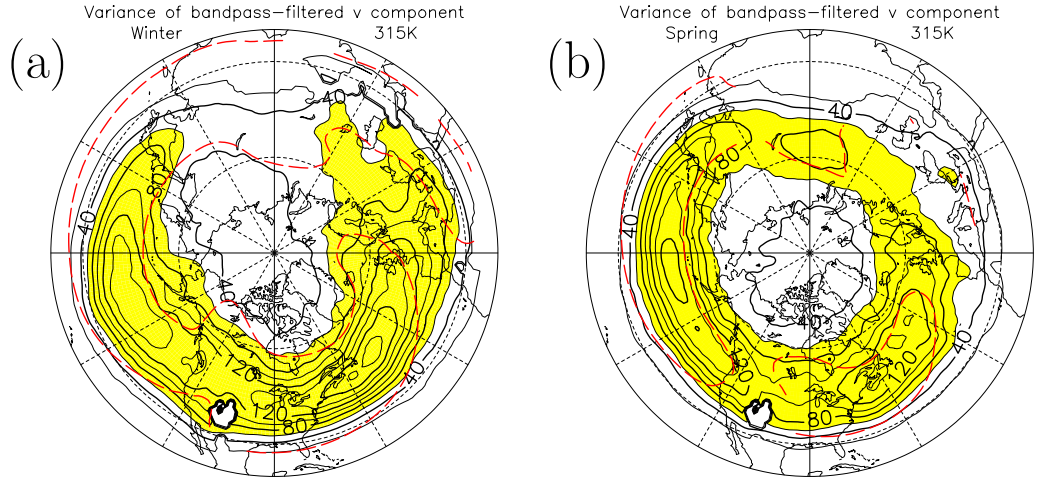

Figure 21. Variances of the bandpass filtered meridional-wind component (unit: $\mathrm{m^2\,s^{-2}}$) at the 315 K isentropic surface in winter (left) and spring (right). Areas with more than $60\,\mathrm{m^2\,s^{-2}}$ are shown in yellow. Red dashed lines indicate the climatological zonal-wind component of $15\,\mathrm{m\,s^{-1}}$. These values are calculated between 2009 and 2014. Values are missing in some regions of low latitudes owing to a lack of data for low potential temperature.

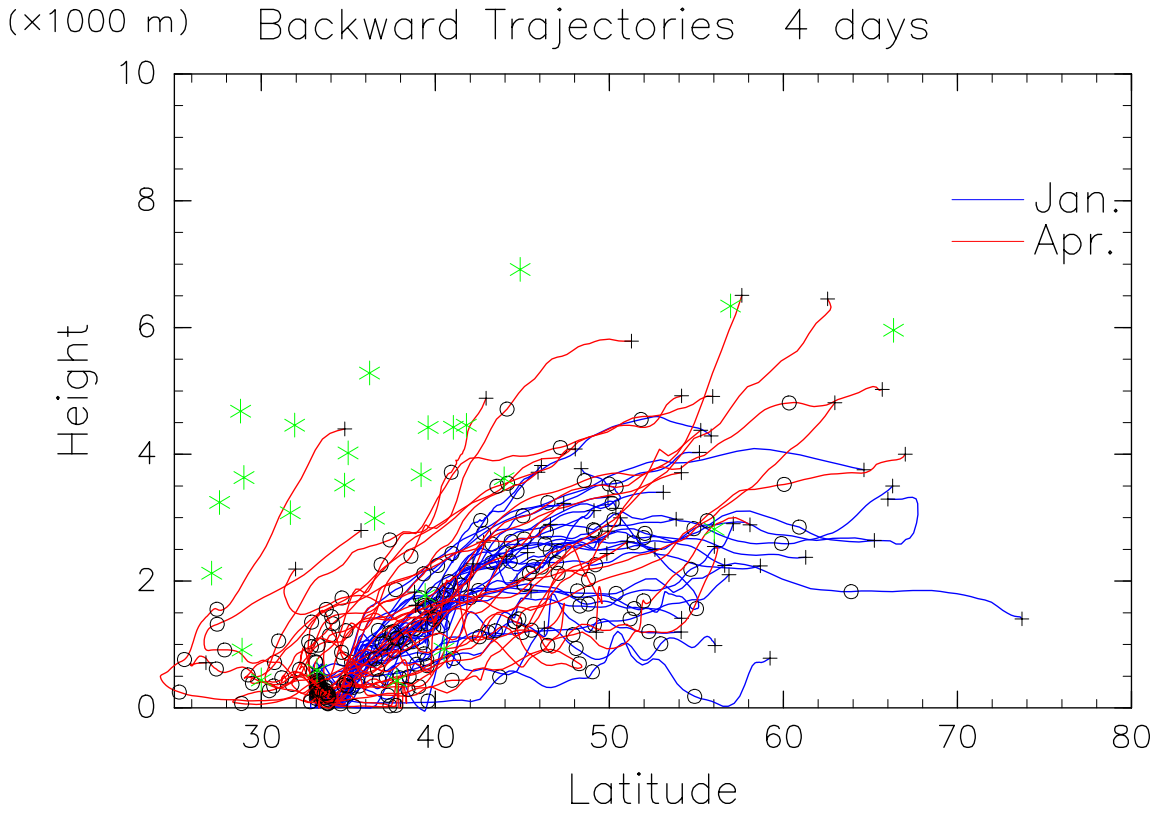

Figure 22. Projections of backward trajectories to the latitude-vertical section for four days from 00:00 UTC on all days in January and April in 2010. The ∘ and + symbols indicate positions at 00:00 UTC. The green star marks represent the parcels on four days before the starting time on the trajectories that show the highest altitude for all 33 cases.

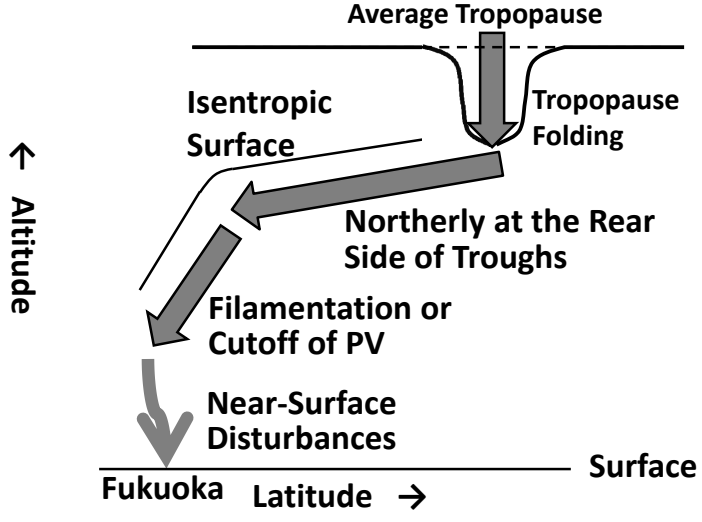

Figure 23. Schematic diagram of the descent from high latitudes.